nature

https://doi.org/10.1038/s41586-023-05948-2

Accelerated Article Preview

Adeno-associated virus 2 infection in children with non-A-E hepatitis

Received: 21 July 2022

Accepted: 10 March 2023

Accelerated Article Preview

Cite this article as: Ho, A. et al. Adeno-associated virus 2 infection in children with non-A-E hepatitis. *Nature* https://doi.org/10.1038/s41586-023-05948-2 (2023)

Antonia Ho, Richard Orton, Rachel Tayler, Patawee Asamaphan, Vanessa Herder, Chris Davis, Lily Tong, Katherine Smollett, Maria Manali, Jay Allan, Konrad Rawlik, Sarah E. McDonald, Elen Vink, Louisa Pollock, Louise Gannon, Clair Evans, Jim McMenamin, Kirsty Roy, Kimberly Marsh, Titus Divala, Matthew T. G. Holden, Michael Lockhart, David Yirrell, Sandra Currie, Maureen O'Leary, David Henderson, Samantha J. Shepherd, Celia Jackson, Rory Gunson, Alasdair MacLean, Neil McInnes, Amanda Bradley-Stewart, Richard Battle, Jill Hollenbach, Paul Henderson, Miranda Odam, Primrose Chikowore, Wilna Oosthuyzen, Meera Chand, Melissa Shea Hamilton, Diego Estrada-Rivadeneyra, Michael Levin, Nikos Avramidis, Erola Pairo-Castineira, Veronique Vitart, Craig Wilkie, DIAMONDS consortium, ISARIC4C investigators, Massimo Palmarini, Surajit Ray, David L. Robertson, Ana da Silva Filipe, Brian J. Willett, Judith Breuer, Malcolm G. Semple, David Turner, J. Kenneth Baillie & Emma C. Thomson

Adeno-associated virus 2 infection in children with non-A-E hepatitis

Antonia Ho[1,211], Richard Orton[1,211], Rachel Tayler[2,211], Patawee Asamaphan[1,211], Vanessa Herder[1,211], Chris Davis[1,211], Lily Tong[1], Katherine Smollett[1], Maria Manali[1], Jay Allan[1], Konrad Rawlik[3], Sarah E. McDonald[1], Elen Vink[1], Louisa Pollock[2], Louise Gannon[4], Clair Evans[5], Jim McMenamin[6], Kirsty Roy[6], Kimberly Marsh[6], Titus Divala[6], Matthew TG Holden[6], Michael Lockhart[6], David Yirrell[6], Sandra Currie[6], Maureen O'Leary[6], David Henderson[6], Samantha J. Shepherd[7], Celia Jackson[7], Rory Gunson[7], Alasdair MacLean[7], Neil McInnes[7], Amanda Bradley-Stewart[8], Richard Battle[9], Jill Hollenbach[10], Paul Henderson[11], Miranda Odam[3], Primrose Chikowore[3], Wilna Oosthuyzen [3], Meera Chand[12], Melissa Shea Hamilton[13], Diego Estrada-Rivadeneyra[13], Michael Levin[13], Nikos Avramidis[3], Erola Pairo-Castineira[3], Veronique Vitart[3,14], Craig Wilkie[15], DIAMONDS consortium*, ISARIC4C Investigators*, Massimo Palmarini[1], Surajit Ray[15], David L. Robertson[1,212], Ana da Silva Filipe[1,212], Brian J. Willett[1,212], Judith Breuer[16,212], Malcolm G. Semple[17,212], David Turner[9,212], J Kenneth Baillie[3,13,212] & Emma C. Thomson[1,18,212]†

1. Medical Research Council-University of Glasgow Centre for Virus Research, Glasgow, United Kingdom
2. Department of Paediatrics, Royal Hospital for Children, Glasgow, United Kingdom
3. Pandemic Science Hub, Centre for Inflammation Research and Roslin Institute, University of Edinburgh, Edinburgh, United Kingdom
4. Department of Paediatrics, NHS Tayside, United Kingdom
5. Department of Pathology, Queen Elizabeth University Hospital, Glasgow, United Kingdom
6. Public Health Scotland, Glasgow, United Kingdom
7. West of Scotland Specialist Virology Centre, Glasgow, United Kingdom
8. Virology Laboratory, Ninewells Hospital, Dundee, United Kingdom

9. Histocompatibility and Immunogenetics (H&I) Laboratory, Scottish National Blood Transfusion Service, Edinburgh Royal Infirmary, Edinburgh, United Kingdom
10. University of California, San Francisco, USA
11. Department of Child Life and Health, University of Edinburgh, United Kingdom
12. United Kingdom Health Security Agency, United Kingdom
13. Section of Paediatric Infectious Disease, Department of Infectious Disease, Imperial College London, London, United Kingdom
14. MRC Human Genetics Unit, Institute for Genetics and Cancer, University of Edinburgh, United Kingdom
15. School of Mathematics and Statistics, University of Glasgow, Glasgow, United Kingdom
16. University College London, London, United Kingdom
17. Pandemic Institute, University of Liverpool, Liverpool, United Kingdom
18. Department of Clinical Research, London School of Hygiene and Tropical Medicine, London, United Kingdom

[211]These authors contributed equally to this work: Antonia Ho, Richard Orton, Rachel Tayler, Patawee Asamaphan, Vanessa Herder, Chris Davis

[212]These authors jointly supervised this work: David L. Robertson, Ana da Silva Filipe, Brian J. Willett, Judith Breuer, Malcolm G. Semple, David Turne, J Kenneth Baillie, Emma C. Thomson

*A list of authors and their affiliations appears at the end of the paper.

†e-mail: emma.thomson@glasgow.ac.uk

An outbreak of acute hepatitis of unknown aetiology in children was reported in Scotland in April 2022[1] and has now been identified in 35 countries[2]. Several recent studies have suggested an association with human adenovirus (HAdV), a virus not commonly associated with hepatitis. Here we report a detailed case-control investigation and find an association between adeno-associated virus (AAV2) infection and host genetics in disease susceptibility. Using next-generation sequencing (NGS), reverse transcription-polymerase chain reaction (RT-PCR), serology and *in situ* hybridisation (ISH), we detected recent infection with AAV2 in the plasma and liver samples of 26/32 (81%) hepatitis cases versus 5/74 (7%) of controls. Further, AAV2 was detected within ballooned hepatocytes alongside a prominent T cell infiltrate in liver biopsies. In keeping with a CD4+ T-cell-mediated immune pathology, the Human Leucocyte Antigen (HLA) class II DRB1*04:01 allele was identified in 25/27 cases (93%), compared with a background frequency of 10/64 (16%; $p=5.49 \times 10^{-12}$). In summary, we report an outbreak of acute paediatric hepatitis associated with AAV2 infection (most likely acquired as a coinfection with HAdV which is required as a "helper virus" to support AAV2 replication) and HLA class II-related disease susceptibility.

In April 2022, several hospitals in Scotland reported that children were presenting to medical practitioners with acute severe hepatitis of unknown aetiology (Fig. 1a)[1]. Elsewhere in the United Kingdom, 270 similar presentations were subsequently reported, for which 15 children required liver transplantation[3]. The World Health Organisation (WHO) have now registered over 1010 probable cases fulfilling their case definition in 35 countries[2]. Understanding the underlying cause of this new disease is a global public health imperative.

Detailed clinical investigations, carried out as part of the public health response, excluded common causes of acute hepatitis including viral hepatitis, drug toxicity and autoimmune hepatitis. Unexpectedly, as it is not a common cause of hepatitis, recent or active human adenovirus (HAdV) infection was identified in Scotland, England and the USA in a high proportion of cases[4-6]. An increase in HAdV diagnoses in Scotland directly preceded the outbreak of unexplained hepatitis in children of a similar age (Fig. 1a,b). SARS-CoV-2 had been circulating for two years and peaked several months before the rise in hepatitis cases (Fig. 1c)[3]. Human herpesvirus 6 (HHV6A and HHV6B) infections were not detected at higher levels during 2021 or 2022 (Fig. 1d).

Research investigation

To investigate the aetiology of the acute hepatitis cases, we recruited 32 affected children, who presented to hospital between 14 March and 20 August 2022 and met the Public Health Scotland (PHS) case definition criteria for inclusion in the International Severe Acute Respiratory and Emerging Infections Consortium (ISARIC) WHO Clinical Characterisation Protocol United Kingdom (CCP-United Kingdom) [ISRCTN 66726260][7]. Control samples were obtained from the Diagnosis and Management of Febrile Illness using RNA Personalised Molecular Signature Diagnosis study cohort (DIAMONDS) and from the NHS Greater Glasgow & Clyde (GG&C) Biorepository, under appropriate ethical approvals (**Methods**)

Clinical presentation

The median age of affected patients was 4.1 years (interquartile range (IQR), 2.7 to 5.5 years) (Table 1). Twenty-one of the 32 (66%) children were female, and all were of white ethnicity. Eighteen (56%) of the children reported a subacute history 2-12 weeks prior to acute hepatitis, characterised by an initial gastroenteritis-like illness followed by intermittent vomiting,

abdominal pain and fatigue. The majority (23/32) had no other medical conditions: one child had previously received a liver transplant; none of the other cases were immunocompromised and none had received COVID-19 vaccination. All routine blood tests for viral hepatitis, including hepatitis A, B, C, E, acute Epstein-Barr virus (EBV), cytomegalovirus (CMV), human herpes virus (HHV) 6/7 and herpes simplex virus (HSV) were negative (Supplementary Table 1). Four cases had low titre (1:80) anti-nuclear antibodies (ANA), and 3 cases low titre (1:40) anti-smooth muscle antibodies (ASMA) but other markers of autoimmunity were negative (Table 1; Supplementary Table 2).

Following hospitalisation, liver biopsies were obtained from five children and revealed evidence of lobular hepatitis with periportal and interface inflammation, intracellular inclusions, bile duct proliferation and ballooning of hepatocytes of varying severity (Fig. 1e-t). Mild to moderate fibrotic changes were noted with no evidence of confluent fibrosis, and there was an inflammatory infiltrate including Major Histocompatibility Complex (MHC) class II-expressing cells. Modified hepatic activity index scores (Ishak)[8,9] ranged from 6 to 11 (Extended Data Table 1) and the biopsies stained negative for complement.

Four cases required transfer to a specialist liver unit due to significant synthetic liver dysfunction. Two of these were treated with steroid therapy and improved. One received supportive care only and improved spontaneously. The fourth severe case required liver transplantation and was treated with cidofovir for HAdV viraemia and steroids post-transplant. The remaining 28 patients received supportive care only with no antiviral or steroid treatment and all showed gradual resolution of hepatitis over 2-3 months. There were no deaths. The median duration of hospital stay was 6 days (range 1-68 days) (Table 1). In the patients with

weakly positive autoantibodies, all had normal or normalising transaminases at last follow up in the absence of anti-inflammatory or immunosuppressive treatment.

Pathogen detection by sequencing

As the epidemiology was in keeping with the emergence of an infectious pathogen, we undertook metagenomic and target enrichment (TE) next generation sequencing (NGS) on all available clinical samples from the first nine recruited patients, including plasma (n=9), liver biopsies (n=4), throat swabs (n=6), faecal samples (n=7) and a rectal swab (n=1), with an average of 14 million sequence reads per sample (Fig. 2a-d;). These were obtained between 7-80 days after initial symptom onset. Control subjects were restricted to children recruited in the United Kingdom between January 2020 and April 2022. Two comparison groups were identified: Group 1, serum or plasma from 13 age-matched healthy children (10 male, 3 female; age range 3-5 years) and Group 2, serum or plasma from 12 children (8 male, 4 female; age range 1-4 years) with PCR-confirmed HAdV infection and normal transaminases (n=12). The Group 2 controls had been diagnosed by nasopharyngeal aspirate (n=10), by nose swab (n=1) and by stool (n=1) as part of routine clinical investigation and half had required critical care. There was no significant difference in age between hepatitis cases and Group 1 healthy controls, but some control samples were sampled earlier than case samples (January 2020-April 2022 versus March-April 2022) (Extended Data Table 2a). Group 2 controls were younger (median age 1.4 years; interquartile range (IQR) 1.1-3.1 years, $p<0.001$) and were collected between May 2020 and December 2021 (Extended Data Table 2b). Metagenomic NGS was carried out using protocols designed to identify both RNA and DNA viruses. Semi-agnostic TE sequencing was also performed using VirCapSeq-VERT Capture probes that target the genomes of 207 viral taxa known to infect vertebrates.

TE sequencing reflected metagenomic NGS results but with higher sensitivity and correlated with viral load measured by qRT-PCR (Supplementary Fig.s 1,2). By both methods, the viral genome detected most frequently in affected patient plasma was adeno-associated virus 2 (AAV2) in 9/9 cases (Fig. 2a; Supplementary Table 3; Extended Data Fig. 1). AAV2 was also detected in 4/4 liver biopsies, and in 1/7 faecal, 1/1 rectal and 1/6 throat swab samples. At lower read counts, HAdV-F41 or HAdV-C were detected in 6/9 patients, while HHV6B was detected in 3/4 plasma samples (Extended Data Fig. 1; Supplementary Tables 4, 5; Supplementary Fig. 3). HAdV types C1, 2, 5 and 6 could not be reliably distinguished due to low read counts. The remaining clinical samples were excluded from analysis for HHV by sequencing because murine herpesvirus 1 (MHV1) had been added as an extraction control during routine clinical investigation.

Read counts of AAV2 by TE were high (median 4478 reads/million; IQR 774-10,498 reads/million) in all 9/9 hepatitis cases versus 0/13 Group 1 healthy controls (IQR 0-0 reads/million; $p<0.001$) and 0/12 Group 2 controls (HAdV-infected children with normal LFTs; IQR 0-0 reads/million; $p<0.001$) (Supplementary Table 5). HAdV reads were detected in 6/12 Group 2 HAdV-positive controls (median 0.82 reads/million, IQR 0-1053 reads/million) despite plasma/sera being a suboptimal sample type to detect HAdV, and in 3/9 cases (median 0 reads/million; IQR 0-0.6 reads/million), more than in 0/13 Group 1 healthy controls (IQR 0-0 reads/million; $p=0.055$). HHV6B was also detected in 3/4 hepatitis cases versus 0/13 healthy controls (median 1.9 reads/million, IQR 0.3-3.5 reads/million and IQR 0-0 reads/million; $p=0.006$, respectively) (Supplementary Table 4). However, HHV6B read counts did not differ significantly between hepatitis cases and Group 2 controls (median 0; IQR 0-0.04 reads per million; $p=0.16$), in keeping with reactivation of HHV6B in the context of severe illness. While metagenomic and TE sequencing from the 13 age-matched healthy

control samples (Group 1) revealed no evidence of AAV2, HAdV or HHV6B in plasma, low read counts of EBV, CMV and HHV6A were detected in a small number of samples (Supplementary Table 4). In Group 2 (HAdV infection and normal LFTs), herpesviruses were detected in 9/12 samples, including 2/12 (as described above) with detectable numbers of HHV6B reads (1050 and 5062 reads/million respectively), confirmed by PCR.

Sequence and phylogenetic analysis

Near-full genomes of AAV2 were obtained from all 9 affected patients (accession numbers OP019741-OP019749) and in all cases, two large open reading frames corresponding to the *rep* and *cap* genes, flanked by ITR regions, were identified. Seven distinct sequences of AAV2 were noted (Extended Data Fig. 2), forming a single clade with 4 AAV2 genomes detected in France between 2004 and 2015. Two of three identical sequences were known to have come from the same household so are almost certainly linked epidemiologically, while the third occurred around the same time but was not known to be linked to the other cases. Sequences from the liver matched those detected in plasma. Several mutations within the VP1-3 genes were noted to be over-represented in the sequences derived from patients with hepatitis when compared with reference sequences (Extended Data Fig. 2). Notably, 9 of the capsid gene mutations over-represented in hepatitis cases (V151A, R447K, T450A, Q457M, S492A, E499D, F533Y, R585S and R588T) are associated with an AAV2 variant that has an altered phenotype, including substantial evasion of neutralising antibodies directed against wild-type AAV2, enhanced production yields, reduced heparin binding, increased virion stability and more localised spread in a mouse model[10 8 9].

A full genome of HAdV-F41 was obtained from a faecal sample (accession number OP019750) and was found to be closest phylogenetically to two genomes reported from Germany in 2019

and 2022 (Extended Data Fig. 2). Contigs matching to other human pathogens, including human coronavirus NL63, rhinovirus C, enterovirus B, human parainfluenza virus 2 and 3, norovirus, and both beta- and gammaherpesviruses were also detected across cases, albeit not consistently. These findings were confirmed by PCR (Supplementary Table 1).

Confirmatory PCR testing of cases 1-9

PCR testing for AAV2 was positive in all 9 cases. Standards were used to estimate viral load of positive samples (Supplementary Fig. 2). All 9 plasma samples tested negative by PCR for HHV6, HSV, CMV and EBV. Two of the four liver biopsy specimens tested positive for HHV6 (cycle threshold (Ct) 33 and 36) (Supplementary Table 1). HAdV was detected in 3/9 plasma samples, 3/4 liver biopsies, 2/6 throat swabs, 4/7 faecal samples and 1/1 rectal swab. The lower detection of HAdV and HHV6 by PCR compared to enrichment sequencing likely reflects a slightly lower sensitivity of the PCR assay. The low numbers of HAdV-positive samples detected using both assays may reflect plasma being a suboptimal sample type for HAdV detection (whole blood samples were unavailable).

Case control study

To investigate the presence of AAV2 and the candidate helper viruses HAdV and HHV6B in plasma samples from the hepatitis cases, we undertook a case-control study, comparing 32 hepatitis cases with the Group 1 and 2 controls described above, and two additional control groups (Fig. 2a-f). Group 3 controls, 33 children (18 males and 15 females aged 2-16 years) with raised transaminases who were HAdV PCR negative, were used to test the hypothesis that reactivation of AAV2 may occur in children with severe hepatitis and may be a correlate of liver dysfunction. These children were older (median age 10.2 years; IQR 7-13.6 years,

p<0.001) than the study cases (Extended Data Table 2b) and 15/33 had required critical care for ventilatory or cardiovascular support. Group 4 controls, residual plasma/serum from 16 Scottish children aged 10 and under attending hospital contemporaneously with the hepatitis cases between March and April 2022, were used to determine whether AAV2 was circulating widely in children in healthcare facilities across Scotland at the time the hepatitis cases were admitted to hospital. Clinical details, including liver function were not available in this group. To ensure the quantification of the AAV2 was performed accurately, we confirmed standard curve concentrations using droplet digital PCR (ddPCR; Methods).

Significance differences between groups for viral loads in plasma were calculated using the Mann-Whitney test (two-tailed). AAV2 qRT-PCR of plasma from 26/32 cases was positive with a median estimated copy number of 66,100 copies/ml (IQR 13,461- 300,277 copies/ml), higher than all control groups (p<0.001 for all case-control comparisons). The median copy number in control Groups 1-3 was below the detection limit. A median of 3,268 copies/ml, (detection threshold of 3,200 copies/ml) was present in control Group 4 suggesting that AAV2 was circulating at low level in children during March and April 2022 (Fig. 2c;). Although five plasma samples from hepatitis cases were HAdV-positive by PCR, and one tested positive by PCR for HHV6 DNA, these results were not significantly more common than in control samples (Supplementary Fig. 3).

Next, five liver biopsies from hepatitis cases were compared with 19 control residual liver biopsies from children under 18 years old. The median AAV2 viral load was 3,721,497 copies/mm^3 of liver (IQR 3,308,243 -6,717,616 copies/ mm^3) in hepatitis cases, and 64 copies/mm^3 of liver (IQR 20-83 copies/mm^3) in controls; p<0.001 (Fig. 2d). Glyceraldehyde-3-phosphate dehydrogenase (GAPDH) was used as a marker of extraction efficiency in all

samples and was similar in case and control samples. When outliers were removed, statistical significance was retained (Supplementary Fig. 4).

Longitudinal sampling

To investigate AAV2 viraemia and liver function over time, longitudinal PCR testing was performed in 14 cases from whom multiple retrospective plasma samples were available (Supplementary Fig. 5). Spearman's rank correlation coefficients for the relationships between the trajectories of viral load and ALT and bilirubin were positive for most cases. However, overall statistical significance could not be confirmed due to sample size.

Where samples were available, we screened for the presence of AAV2-specific IgM and IgG within patient samples and Groups 1 and 4 healthy and contemporaneous controls (Fig. 2e,f; Supplementary Fig. 6). Anti-AAV2 IgM was detected in 15/23 (65.2%) of hepatitis cases, but only 1/13 Group 1 healthy control samples (7.7%) and 2/16 (12.5%) Group 4 Scottish contemporaneous controls, respectively. For the case samples that tested negative for AAV2-specific IgM, four patients were noted to be fewer than three days post-onset of illness and two patients were more than 77 days post-illness onset. IgG was detected in 21/23 (91.3%) of cases, in 8/13 (61.5%) of age-matched healthy controls and in 9/16 (56.3%) of Scottish healthy controls. Of the two seronegative patients, both were early time points, likely sampled prior to expected seroconversion (less than 3 days after the onset of illness).

SARS-CoV-2 infection

Routine clinical investigation detected SARS-CoV-2 nucleic acid in nasopharyngeal samples from only 3/31 (9.6%) children at the time of illness, two of whom were also seropositive. The

third became infected after the onset of hepatitis. SARS-CoV-2 was not detected by PCR or by sequencing in any of the case or control samples available for analysis, including liver samples. Nevertheless, to investigate the possibility that unexplained hepatitis in children might relate to a prior infection with SARS-CoV-2 or other seasonal coronaviruses, we carried out serological analysis of 23 available residual samples from cases. IgG antibody titres were measured quantitatively against SARS-CoV-2 spike (S) protein, N-terminal domain (NTD) and receptor binding domain (RBD) of spike, and nucleocapsid (N), and the human seasonal coronaviruses (HCoVs) 229E, OC43, NL63 and HKU1. Electrochemiluminescence assay (MSD-ECL) for coronavirus-specific IgG revealed prior exposure to seasonal coronaviruses; with strong responses detected against NL63 (17/23) and OC43 (21/23) (Extended Data Fig. 3a). In comparison, plasma from 12/23 children displayed high reactivity against HKU1 while only 3/23 reacted strongly against 229E. Plasma from eleven children reacted with two or more SARS-CoV-2 antigens; N, S, NTD or RBD. A single additional child reacted solely with N, indicating that in total, 12/23 displayed serological evidence of prior exposure to SARS-CoV-2 (Extended Data Fig. 3b). In summary, 12/23 (52%) of the children displayed evidence of prior exposure to SARS-CoV-2; a lower level than SARS-CoV-2 seroprevalence in children aged 5-11 years in Scotland between 14th March and 27th June 2022 (when PHS enhanced surveillance for COVID-19 was discontinued), reported as between 59.0% (95% CI 50.6-71.2) and 72.4% (53.9-78.8)[10], indicating no direct link between COVID-19 and the outbreak of acute hepatitis.

Host genetics and HLA typing

To investigate whether some children might be genetically more susceptible to non-A-E hepatitis, 27 cases and 64 Scottish platelet apheresis donor local controls were genotyped using high resolution typing for all HLA loci (HLA-A, B, C, DRB1, DRB3/4/5, DQA1, DQB1,

DPA1 and DPB1). 25/27 (92.6%) of affected patients were positive for at least one copy of the DRB1*04:01 allele versus 10/64 (15.6%) of controls; allele frequency in patients was 0.54 versus 0.08 in controls (OR 13.7 (95% CI 5.5-35.1), p= 5.49 x 10^{-12}). The frequency of the DRB1*04:01 allele (based on imputation of HLA alleles) in a control set of unrelated United Kingdom Biobank participants (n=29,379) was found to be 0.11 (2,942/29,379 allele carriers, OR 112.3 (95% CI 26.6 – 474.5), p=3.27x10^{-23}) and in British/Irish North-West European (BINWE) individuals on the Anthony Nolan charity register, the allele frequency of DRB1*04:01 is also 0.11[10]. To check for cryptic relatedness among patients and population stratification, we performed genome-wide microarray genotyping in 19 cases and excluded participants with a conservative relatedness threshold (identity-by-state >0.4). Comparing to well-matched participants in the United Kingdom Biobank (Extended Data Fig. 4**)**, similar signals for association with disease by allele frequency (p=8.96 x 10^{-6}) and across the three possible biallelic genotypes at this locus (p=1.2 x 10^{-9}) were obtained.

In addition to the DRB1 association, 23/27 patients were positive for DQA1*03:03 versus 11/64 controls (allele frequency 0.54 vs 0.09, odds ratio (OR) 12.3 (5.1-30.7), p = 1.9 x 10^{-11}) and 26/27 patients were positive for DRB4*01:03 versus 21/64 controls (allele frequency 0.67 vs 0.17 OR 9.4 (4.4-21.3), p = 1.8 x 10^{-10}). Due to strong linkage disequilibrium in this region of the genome, it is not possible to be certain which is the causal susceptibility allele.

In situ hybridisation and immune typing

To investigate the presence of AAV2, HAdV and HHV6 in liver biopsies, we carried out *in situ* hybridisation (ISH). Liver biopsies of all patients were characterised by AAV2 RNA within the nuclei and cytoplasm of "ballooned" hepatocytes and in arterial endothelial cells indicating the presence of replicating virus (Fig. 3a-h). AAV2 positive cells were quantified at

high level in all cases using QuPath in biopsies of 5 non-A-non-E hepatitis, ranging from 1.2 to 4.7%. This level is similar to that seen in hepatitis associated with other viruses[11,12]. Consistent with low levels of HHV6B and HAdV sequence reads present in the case biopsies, negligible levels of viral RNA from these viruses were detected by ISH.

To investigate the possibility of an immune-mediated pathogenesis of disease in the liver, multiplex analysis of liver samples was carried out using CO-Detection by indEXing (CODEX) for a variety of immune cellular markers including CD3, CD4, CD8, PD-L1, CD107a, CD20, CD31, CD44, CD68, Mx1 and PanCK (Fig. 4a-d; Supplementary Fig. 7,8). In the explant liver of patient CVR35, prominent disordered proliferation of epithelial cells throughout the liver tissue was evident, with increased CD68+ macrophages, activated CD4+ and CD8+ T cells, as well as CD20+ B cells. High expression of the interferon-induced GTP-binding protein Mx-1 was also noted, indicating activation of the innate immune response[13].

Conclusions/final statements

In this study, we report the association of AAV2 and the class II HLA allele DRB1*04:01 with an outbreak of paediatric non-A-E hepatitis, virus being detected independently by sequencing, real-time PCR and *in situ* hybridisation. Liver tissue from biopsies of all patients was characterised by AAV2 RNA (indicating replicating virus) within the nucleus and cytoplasm of "ballooned" hepatocytes and by a dense CD4+ and CD8+ infiltrate in the liver with an activated phenotype. A CD4+ T-helper cell-mediated immunopathological response triggered by exposure to AAV2 infection is highly likely, consistent with the markedly increased frequency of the MHC class II DRB1*04:01 allele in affected children.

AAV2 is a small non-enveloped virus with a single-stranded DNA genome of around 4,675 nucleotides in length belonging to the species adeno-associated dependoparvovirus A (genus Dependoparvovirus, family Parvoviridae).[14] It was first described in 1965 and infects up to

80% of the adult population. Seroconversion occurs in early childhood following respiratory infection[15]. In a prospective study in the USA, the earliest seroconversion to AAV2 infection occurred in a 9-month-old child and its seroprevalence increased from 24.2% to 38.7% in 3 and 5-year-old children, respectively[16]. This age range coincides with that of the cases in this study, suggesting that illness may be related to primary infection with AAV2 rather than its reactivation. In line with this hypothesis, we demonstrated anti-AAV2 IgM reactivity in the majority of affected children. AAV2 relies on coinfection with a helper virus for replication, most commonly HAdV or a herpesvirus. Most clinical samples taken at presentation with hepatitis were obtained more than 20 days after initial symptom onset, which could explain the absence of a helper virus in some samples, and low viral loads in positive samples. In an exploratory study using NGS, we detected two candidate helper viruses at low level in the hepatitis cases: HAdV and HHV6B (6/9 and 3/9 cases respectively). These viruses were not confirmed to be higher in cases than controls in plasma or liver samples in our larger case-control study; HHV6B was also present in two control groups that included children with severe HAdV infection and children with hepatitis of alternative aetiology. As HHV-6 can establish latency and can integrate its genome into the human chromosome, it may reactivate following concomitant illness (or immunosuppression) and may represent either an opportunistic bystander or a pathogen.

We hypothesise that AAV2 is directly implicated in the pathology of the 2022 outbreak of non-A-E hepatitis in children, following transmission as a co-infection with HAdV or less likely due to reactivation following HAdV or HHV6 infection. Our results also support an association between an HLA class II haplotype and disease susceptibility. A CD4+ T-cell-mediated response may direct a maladaptive T cytotoxic or B cell-mediated immunopathology. In support of this, a CD8+ cell-mediated response directed against the AAV2 viral capsid (VP1) in association with hepatitis was reported in early trials of AAV2 when used as a vector for

gene therapy[17-19]. Hepatitis remains a common phenomenon in AAV-vectored gene therapy, usually treated pre-emptively with steroids before and for several weeks after treatment, and in rare cases has been associated with deaths from fulminant hepatic failure[20,21]. As a result of this investigation, further studies to investigate HLA association with severe illness in gene therapy recipients are indicated. Importantly, we did not find features of autoimmune hepatitis (AIH) in affected children, by serology or histology. In a recent cohort of Scottish children with AIH, the majority had evidence of seropositive disease (100% of patients with type II AIH tested positive for anti-LKM1). Further, AIH patients were older in age (median age 11.4yrs vs. 4.1yrs in our cohort) and had significantly lower median ALT at diagnosis (444 IU/L versus 1756 IU/L). None improved without treatment.[22]

An alternative explanation is that AAV2 is not directly involved in pathology and is rather a biomarker of infection with HAdV. Over half of our cases had subacute symptoms, with a median onset of 42 days before the onset of jaundice. The opportunity to detect virus by sequencing was therefore reduced, as samples were collected after this stage of illness. Further, whole blood samples would have been likely to increase the sensitivity of detection, but only serum/plasma samples were available. We consider this alternative hypothesis to be less likely because we did not detect AAV2 in a control group of children with HAdV infection who had normal liver function. However, HAdV41 is a common cause of diarrhoea in young children[23] and co-infection of AAV2 with HAdV41 may explain early gastrointestinal symptoms in affected children. In contrast, although adenovirus-associated hepatitis has been described, particularly among immunocompromised individuals,[24] HAdV41 has not previously been associated with severe hepatitis. In the recent outbreaks of unexplained hepatitis in children, it has been associated inconsistently[4-6,25-27].

We also investigated the possibility that unexplained cases of hepatitis were linked to prior COVID-19 infection. Direct SARS-CoV-2 liver injury is unlikely, since few of our hepatitis cases (3 of 31) were SARS-CoV-2 PCR-positive on admission, and we did not identify SARS-CoV-2 by PCR or sequencing in any of the clinical samples from cases, including liver biopsies. Further, the SARS-CoV-2 seroprevalence in hepatitis cases was lower than community cases at that time.[3] This is in keeping with a case-control analysis by United KingdomHSA that found no difference in SARS-CoV-2 PCR positivity between hepatitis cases and children presenting to emergency departments between January and June 2022.[3] Nevertheless, we cannot at this time fully exclude a post-COVID-19 immune-mediated phenomenon, for example a link to HLA class II type, in susceptible children.

There are several limitations to this study. Firstly, the presence of AAV2 in hepatitis cases but not Group 1-3 controls may have arisen due to seasonal variation in AAV2 transmission, as some controls were sampled earlier than cases. We included a contemporaneous control group (Group 4) to address this possibility. Low viral loads of AAV2 were detected in a small number of Group 4 control subjects in keeping with the presence of the circulating virus in children at the time the cases occurred. Secondly, the presence of AAV2 in cases is an association and may not represent direct aetiology; rather the AAV2 may be a useful biomarker of recent HAdV (or less likely HHV6B) infection. We do not consider it likely that AAV2 simply represents a marker of liver damage because it was not present in cases of severe hepatitis of alternative aetiology and significantly, we detected AAV2 in ballooned hepatocytes by ISH. The strong association of the HLA-DRB1*04:01 allele, known to be associated with autoimmune[28] and extra-articular manifestations of rheumatoid arthritis[29] supports a strong host genetic impact on susceptibility. This analysis is affected by strong linkage disequilibrium and larger studies are required to confirm the definitive allele association. The HLA association and the presence of

an activated T cell infiltrate alongside AAV2-infected cells in the liver is in keeping with a CD4+-mediated immune pathology[30]. We consider autoimmune disease to be less likely due to the absence of autoantibodies in affected cases and the absence of typical histology in liver specimens. It is also plausible that simultaneous HAdV infection, with a coinfecting or reactivated AAV2 infection has resulted, for a proportion of children who are more susceptible (due to the HLA class II allele HLA-DRB1*04:01), in a more severe outcome than might normally be expected for these commonly circulating viruses. Peptide mapping experiments are indicated in future studies to investigate the nature of the HLA class II-restricted T cell response.

The 2022 outbreak of AAV-2 associated paediatric hepatitis that we describe in this study may have arisen because of changes in exposure patterns to AAV2, HAdV and HHV6B as an indirect consequence of the COVID-19 pandemic. The circulation of common human viruses was interrupted in 2020 by the implementation of non-pharmaceutical interventions, including physical distancing and travel restrictions, instituted to mitigate SARS-CoV-2 transmission. Once restrictions were lifted, genetically susceptible children may have had a higher chance of being co-exposed to HAdV and AAV2 for the first time, creating a synchronised wave of severe disease. Larger case-control studies are urgently needed to confirm the role of AAV2 and HLA in the aetiology of unexplained non-A-E paediatric hepatitis. Retrospective testing of samples from sporadic cases of unexplained hepatitis in children is also needed.

Online content Any methods, additional references, Nature Research reporting summaries, source data, extended data, supplementary information, acknowledgements, peer review information; details of author contributions and competing interests; and statements of data and code availability are available at

Table 1. Demographic and clinical characteristics of the 32 cases with unexplained hepatitis.

Demographics	
Age (years)[a]	4.1 (2.7-5.5, 0.9-10.6) years
Sex - female[b]	20 (63%)
Co-morbidity[b]	9 (28%)[c]
Biochemistry	
Peak bilirubin[a] (µmol/l)	82 (36-160, 3-387)
Peak ALT[a] (U/L)	1757 (708-2763, 333-5417)
Peak AST[a] (U/L)	2048 (833-3408, 424-6908)
Peak GGT[a] (U/L)	124 (91-162, 18-720)
Peak INR[a]	1.2 (1.1-1.4, 1.0-2.9)
Peak CRP[a] (mg/L)	5 (3-11, 1-117)
Caeruloplasmin[a] (n=24) (g/L)	0.36 (0.33-0.39, 0.22-0.52)
Key autoimmune parameters	
IgG[a] (g/L)	11.8 (9.9-14.3, 1.5-21.0)
Coeliac screen (TTG antibody) (n=26)	26 normal range
Anti-mitochondrial antibody	32 negative
Anti-smooth muscle antibody (SMA)	29 negative, 3 low positive (1:40)[c]
Anti-liver kidney microsomal (LKM) 1 antibody	32 negative
Anti-nuclear antibody (ANA)	28 negative, 4 weak positive 1:80 titre[c]
Clinical presentation	
Symptoms at presentation[b] • Vomiting • Jaundice • Poor appetite • Lethargy/fatigue • Abdominal pain • Diarrhoea	 22 (69%) 21 (66%) 12 (38%) 10 (31%) 10 (31%) 4 (13%)
Sub-acute symptoms for ≥14 days prior to presentation (n=32)	18 (56%)
Sub-acute symptoms reported (n=18) • Intermittent vomiting • Initial gastroenteritis-like illness • Abdominal pain • Lethargy/fatigue • Poor appetite • Weight loss	 15 (83%) 12 (67%) 9 (50%) 7 (39%) 6 (33%) 6 (33%)
Approximate duration of sub-acute symptoms prior to presentation[ad]	42 (27-52, 14-85) days
Length of hospital stay[ae]	6 (4-10, 1-68) days
Required transfer to tertiary liver unit	4 (12.5%)

Required liver transplant	1 (3%)

a. Median (interquartile range, range); b. number (%) denominator=32 unless otherwise specified. c. See Supplementary Data for additional clinical details. d. n=16 patients with data available e. n=30, one patient long-term inpatient for unrelated condition, one patient identifed and managed as outpatient.

Figure Legends

Fig. 1: Epidemiology and histological appearance of paediatric hepatitis cases in Scottish children. a, The emergence of acute non-A to E hepatitis in children March-September 2022 [3], **b,** Cases of HAdV , **c**, SARS-CoV-2 and **d,** HHV6 in children aged ≤10 years in Scotland January 2019 to September 2022. Diagnoses in children aged ≤5 years are shown in black and 6-10 years in grey. **e-t,** Histopathology of non-A-E hepatitis cases. **e, i, m, q,** Serial sections of formalin-fixed and paraffin-embedded (FFPE) liver tissue sections (one section for each stain per subject) stained with haematoxylin and eosin (H&E) , **f, j, n, r,** reticulin (highlighting structural organisation , and **g, k, o, s** Masson (highlighting collagen fibres). **m-p**, The regular lobular structure of the control healthy liver (145783) is not recognisable in **e-h,** sections collected from CVR35 who was transplanted. **h,** Immunohistochemistry shows an increase of $MHCII^+$ cells in tissues from CVR35 compared to **l, t,** control liver (bars in **e-h** and **m-p** = 400 μm). **i-l,** higher magnifications micrographs of panels **e-l** showing details of liver histopathology. **i,** In CVR35, enlarged (ballooned) and vacuolated hepatocytes (*) are evident compared to hepatocytes with a regular morphology from q**,** control liver (145783; arrow) with a regular sinus (+). **j**, In CVR35,) the reticulin staining shows destruction of the sinus structures and irregularly arranged fibres, while **r,** control liver shows fibres lining the sinus. **k,** In CVR35, Masson staining shows an increase of collagen fibres (in blue; *) as opposed to minimal staining of fibres (arrow) in a **s,** control liver. **l,** High magnification showing accumulation of $MHCII^+$ cells in the liver (*) of CVR35 while in **t,** control liver , staining is limited to Kupffer cells (bars in **i-Pp** = 50 μm).

Fig. 2: AAV2 detection in paediatric hepatitis cases. a, Heatmap of HAdV and AAV2 reads detected in hepatitis cases by target enrichment sequencing. Samples obtained for routine clinical investigation (plasma, liver, faeces, rectal and throat swab) were

retrospectively sequenced following DNA or RNA extraction. AAV2 read counts are shown from 0 to >100 reads/million in green (upper row) and HAdV read counts are shown from 0 to >10 reads/million in red (lower row). **b,** Heatmap of viral reads from plasma in hepatitis cases and plasma/sera from controls. Plasma samples from hepatitis cases, and plasma or sera samples from children with HAdV infection and age-matched healthy controls were sequenced following DNA or RNA extraction. AAV2 read counts are shown from 0 to >50 reads/million in green and HAdV read counts are shown from 0 to >5 reads/million in red. The number of days between initial symptom onset and sample are indicated. **c,** AAV2 real-time qRT-PCR of serum/plasma in 32 hepatitis cases versus 74 control subjects in four groups (13 in Group 1, 12 in Group 2, 33 in Group 3 and 16 in Group 4). The detection threshold of the assay (3200 copies/ml) is shown as a dotted line. Values are shown as a scatter plot with a median line. Statistical analysis was performed using the Mann-Whitney test (two-tailed). **d,** AAV2 real-time qRT-PCR of liver biopsies in 5 hepatitis cases versus 19 controls. Statistical analysis was performed using the Mann Whitney test (two-tailed). **e,** IgM responses determined by ELISA in 22 hepatitis cases versus 29 controls (13 in Group 3, 16 in Group 4)**f,** IgG responses determined by ELISA in 22 hepatitis cases versus 29 controls (13 in Group 3, 16 in Group 4). Statistical analysis was performed using the Mann Whitney test (two-tailed). Data in panels c-f were carried out in triplicate.

Fig. 3 *In situ* hybridization of AAV2 in liver tissue. In panels **a-h,** RNA *in situ*-hybridisation for the detection of AAV2 RNA in sections of FFPE liver tissues from children (one section per patient) with non A-E hepatitis is shown. In **a,** AAV-2 RNA (red signal, arrows) is detected in the endothelial cells of arteries in an explant liver section from patient CVR35. The vascular lumen is highlighted with an asterisk (*). Positive AAV2 signal is shown in the nuclei of hepatocytes with vacuolated morphology from patient CVR4 (**b**; arrows) andnegative cell (circle). In **c,** a liver section from patient CVR1 shows AAV2 viral RNA both in the nucleus and in the cytoplasm (bar, 50 μm), while in **d** (CVR9), AAV2 RNA is found only in the nucleus. Panel **e** shows a high percentage of hepatocytes with a positive signal for AAV2 predominantly in the nucleus of hepatocytes (CVR1). AAV2 is not detectable in liver sections from control patients (**f**) in either the endothelial cells or hepatocytes (bar of insert and X, 50 μm). In **g**, inclusion bodies from patient CVR35, left panel, small, dark basophilic intranuclear inclusion bodies in hepatocytes next to the nucleolus (arrows); right panel,bottom right corner, a hepatocyte with a large, pale-basophilic, diffuse intranuclear inclusion body (suggestive of adenovirus infection, arrow) next to a multinucleated giant cell in the liver (*). Bars in **a, b, c, d, f and g** = 50μm; Insets in **c** and **d** = 25μm; **e** = 200μm. AAV2 positive cells were quantified using QuPath (**h**) in biopsies of 5 non-A-non-E hepatitis and control patients; patient CVR35 (transplanted) highlighted in red. Using the entire section, cells were segmented to identify the nuclei and cytoplasm, the algorithm was tuned to detect red signa. All samples were analysed using the same algorithm.

Fig. 4 CO-Detection by indEXing (CODEX) analysis of liver tissue. Liver tissue from CVR35 and a control liver sample show differences in the control (a and c) and the patient

(CVR35; b and d) in cellular composition (c, d); bile ducts (*). Regular structured bile ducts in a control liver biopsy (**a**) arehighlighted by * and green staining of epithelial cells using cytokeratin. Scattered macrophages (CD68, red), T cells (CD3, cyan) and activated T cells (CD44, yellow) are also present. In contrast, the explant liver (patient CVR35) in **b** shows prominent proliferation of epithelial cells throughout the liver tissue (green), with increased macrophages (red), T cells (cyan) and activated T cells (yellow). In panel **c**, the control liver shows scattered cytotoxic T (CD8, red), CD107a positive (brown) and CD4 positive (yellow) cells and low expression of the interferon-induced GTP-binding protein Mx-1(green), compared to high numbers of all cell types and high Mx-1 expression in the explant patient **d**. Bars (**a-d**), 50 micrometres. One section of liver was stained per subject, and the entire area was outlined manually. Cells were segmented to identify the nuclei and cytoplasm, and the algorithm was tuned to detect the colour signal in the cells. All samples were analysed with the same algorithm for each stain.

Extended data legends

Extended Data Figure 1 | AAV2, HAdV and human herpesvirus detection by target enrichment sequencing in cases and controls. Read counts per million are plotted for a) HAdV; b) AAV2; c) HHV6B; d) HSV1; e) HSV2; f) VZV; g) HHV6A; h) HHV7; i) HHV8; and j) CMV in cases, Group 1 healthy controls and Group 2 controls (HAdV positive children with normal liver function). Statistical significance was estimated using a Mann-Whitney test (two-sided).

Extended Data Figure 2 | Phylogenetic and sequence analysis of AAV2 genomes. a) Maximum likelihood phylogeny of AAV2 from hepatitis cases CVR1-9. The nine AAV2 genome sequences generated from the plasma samples via target enrichment (highlighted in green) were aligned with a range of the closest AAV GenBank sequences[33]**.** AAV2 reference

sequences are denoted by accession number, country and year of sampling b,) Phylogeny of HAdV41 genome from case 5. The HAdV41 genome sequence from the faecal sample of patient 5 (red) was combined with complete genomes of HAdV41 from GenBank. Bootstrap values >70 are indicated. HAdV41 reference sequences are denoted by accession number, country and year of sampling; c,) Key mutations and hierarchical clustering of AAV2 genomes. Mutations in published AAV2 sequences are highlighted in (blue) and case sequences (green); d) Mutations over-represented in hepatitis cases versus controls. Mutations in VP1-3, Rep78 and 52 and AAP are highlighted by % representation in case sequences (green) and published sequences (blue).

Extended Data Figure 3 | Reactivity of sera from paediatric hepatitis cases against human seasonal coronaviruses and SARS-CoV-2. Sera from the paediatric hepatitis cases were screened for reactivity against spike proteins from **a)** seasonal coronaviruses 229E, OC43, NL63 and HKU1, and **b**) SARS-CoV-2 nucleocapsid (N), spike (S), and N-terminal domain (NTD) and receptor binding domain (RBD) of S by electrochemiluminescence (MSD-ECL). Reactivity of the 23 samples (Hepatitis) was compared with 16 sera from contemporaneous control samples from children (Group 4 Controls), and three groups of sera from adults of known SARS-CoV-2 status; Negatives (never tested positive for SARS-CoV-2; n=30), Vaccinated two doses (n=28) and Infected (n=39).

Extended Data Figure 4 | Principal component analysis (PCA) plots showing the first four genome-wide principal components to confirm genetic ancestry matching. **a)** Genomic PCA using full United Kingdom Biobank cohort as background population (grey), showing the subgroup of unrelated United Kingdom Biobank participants who were born in Scotland

and of Caucasian ancestry (blue) and the hepatitis cases reported here (red). **b)** plots showing only the subgroup born in Scotland and of Caucasian ancestry.

Extended Data Table 1 Modified hepatic activity index scores

Extended Data Table 2 Characteristics of cases and controls a) used in metagenomic and target enrichment analysis b) used in PCR analysis

*Fisher's Exact or chi-squared test for categorical and Mann-Whitney (two-sided) test for continuous variable.

† Age and sex of Group 4 controls unavailable.

Methods

ISARIC CCP-United Kingdom recruitment, Biorepository & DIAMONDS studies

Ethical approval for the ISARIC CCP-United Kingdom study was given by the South Central–Oxford C Research Ethics Committee in England (13/SC/0149), the Scotland A Research Ethics Committee (20/SS/0028), and the WHO Ethics Review Committee (RPC571 and RPC572). Thirty-two children aged <16 years were recruited prospectively by written informed consent (parent or guardian) from the ISARIC WHO CCP-United Kingdom cohort admitted to hospital with elevated transaminases (defined as ALT >400 IU/L and/or AST >400 IU/L) that was not due to viral hepatitis A-E, autoimmune hepatitis or poisoning. Nine cases had available clinical samples for further investigation. Three further cases had HLA typing performed but samples were not available for further analysis. Control samples were obtained from children (aged <16 years) recruited to the Diagnosis and Management of Febrile Illness using RNA Personalised Molecular Signature Diagnosis (DIAMONDS), an ongoing multi-country study that aims to develop a molecular diagnostic test for the rapid diagnosis of severe infection and inflammatory diseases using personalised gene signatures (ISRCTN12394803). Ethical

approval was given by London-Dulwich Research Ethics Committee (20/HRA/1714). Controls included healthy controls (n=13; Group 1), children with PCR-confirmed adenoviral infection with normal transaminases (n=12; Group 2), and children with raised transaminases without adenoviral infection (n=33; Group 3), recruited between 19 May 2020 to 8 January 2022. Scottish surplus plasma (aged <10 years; March to April 2022; Group 4) and liver biopsy control samples (aged <18 years; January 2021-July 2022) from the Diagnostic Pathology/Blood Sciences archive were obtained with NHS GG&C Biorepository approval (application #717; REC 22/WS/0020). Negative control adult samples that had tested negative by PCR for SARS-CoV-2 were used as an additional group for serological analysis of coronaviruses, also with NHS GG&C Biorepository approval. These samples were used without consent following HTA legislation on consent exemption.

Viral PCR

RNA extraction was carried out using the Biomerieux Easymag generic protocol. 300ul of plasma or sera was extracted and eluted into 80 ul of water.

AAV2 qRT-PCR was performed to detect a 62bp amplicon of the AAV2 inverted terminal repeat region (ITR) as previously described[32] using the forward ITR primer 5'-GGAACCCCTAGTGATGGAGTT-3') and the reverse ITR primer 5'-CGGCCTCAGTGAGCGA-3'). The AAV2 ITR hydrolysis probe was labelled with fluorescein (6FAM) and quenched with Black Hole quencher (BHQ) 5'-[6FAM]-CACTCCCTCTCTGCGCGCTCG-[BHQ1]3'). AAV2 primers and probe were synthesised by Merck Life Sciences United Kingdom Limited, United Kingdom. qRT-PCR analysis was performed using the ABI7500 Fast Real-Time PCR system (Applied Biosystems). LUNA

Universal One-Step RT PCR kit (New England Biolabs) was used for the amplification and detection of the AAV2 ITR target. qRT-PCR reactions were performed in a 20µl volume reaction (Luna Universal One-Step reaction mix, Luna WarmStart RT enzyme mix, 400nM forward and reverse primers, 200nM AAV2 ITR probe and 1-2.5µl of template DNA) as per manufacturer's instructions. To quantify the number of copies, serial dilutions of plasmid containing the 62bp ITR product were used to generate a standard curve which was then used to interpolate the copy number of AAV2 copies in the samples. Wells with no template were used as negative controls. qRT-PCR reactions were performed in triplicate. The qRT-PCR program consisted of an initial reverse transcription step at 55 C for 10 minutes, an initial denaturation at 95 C for 1 minute followed by 45 cycles 95 C denaturation for 10 seconds and extension at 58 C for 1 minute. A qPCR detection limit between 31 and 32 cycles was calculated as the threshold Ct value at the last dilution of DNA standards that were within the linear range. A PCR result was considered positive if all three reactions tested positive at $\leq$31 cycles.

Digital droplet PCR (ddPCR) was performed according to the manufacturer's instructions using the ddPCR Supermix for Probes (No dUTP) (Bio-Rad, United Kingdom cat no. 1863023) and analysed using an QX200 Droplet Digital PCR system (Bio-Rad, United Kingdom cat no. 1864001)

The West of Scotland Specialist Virology Centre, NHS Greater Glasgow and Clyde conducted diagnostic real-time PCR with reverse transcription to detect HAdV, SARS-CoV-2-positive samples and other viral pathogens associated with hepatitis (e.g. Hepatitis A-E), following nucleic acid extraction utilizing the NucliSENS easyMAG and Roche MG96 platforms. HHV6[2] and HAdV41[33] were tested by qPCR as previously described using Invitrogen platinum qPCR mix (Cat no 11730-025) and Quanta Biosciences qPCR mix Mastermix (Cat.No. 733-

1273) respectively on an ABI7500 and amplified for 40 cycles. A 6ul extract was amplified in a total reaction volume of 15ul.

Measurement of antibody response to coronaviruses by electrochemiluminescence

IgG antibody titres were measured quantitatively against SARS-CoV-2 spike (S) protein, N-terminal domain (NTD), receptor binding domain (RBD) or nucleocapsid (N), and the spike glycoproteins of human seasonal coronaviruses (HCoVs) 229E, OC43, NL63 and HKU1 using MSD V-PLEX COVID-19 Coronavirus Panel 2 (K15369) and Respiratory Panel 1 (K15365) kits. Multiplex Meso Scale Discovery electrochemiluminescence (MSD-ECL) assays were performed according to manufacturer instructions. Samples were diluted 1:5000 in diluent and added to the plates along with serially diluted reference standard (calibrator) and serology controls 1.1, 1.2 and 1.3. Plates were read using a MESO Sector S 600 plate reader. Data were generated by Methodological Mind software and analysed using MSD Discovery Workbench (v4.0). Results are expressed as MSD arbitrary units per ml (AU/ml). Adult negative and positive pools gave the following values: Negative pool - spike 56.6 AU/ml, NTD 119.4 AU/ml, RBD 110.5 AU/ml and nucleocapsid 20.7 AU/ml; SARS-CoV-2 Positive pool – spike 1331.1 AU/ml, NTD 1545.2 AU/ml, RBD 1156.4 AU/ml and nucleocapsid 1549.0 AU/ml. In the same assay, NIBSC 20/130 reference serum – spike 547.7 AU/ml, NTD 538.8 AU/ml, RBD 536.9 AU/ml and nucleocapsid 1840.2 AU/ml.

Metagenomic sequencing

Full protocols on the discovery of RNA and DNA viruses using metagenomic next-generation sequencing and target enrichment sequencing methods can be found at the following sites:

dx.doi.org/10.17504/protocols.io.261ge34zol47/v1

dx.doi.org/10.17504/protocols.io.36wgqj3q3vk5/v1

In summary, residual nucleic acid from 27 samples (9 patients with a combination of plasma, liver, faeces, rectal and throat/nose samples), 12 HAdV-positive and 13 healthy controls (control samples were either plasma or sera) underwent metagenomic next-generation sequencing at the CVR. Briefly, each nucleic acid sample was split in two library preparations, to improve the chances of detecting RNA and DNA viruses. The protocol applied for improved detection of RNA viruses included treatment with DNaseI (Ambion DNase I, ThermoFisher), ribosomal depletion (Ribo-Zero Plus rRNA Depletion Kit, Illumina), except for plasma samples, reverse transcription (SuperScript III, Invitrogen) and double-strand DNA synthesis (NEBNext® Ultra™ II Non-Directional RNA Second Strand Synthesis Module, NEB). The protocol applied to detect DNA viruses included partial removal of host DNA (NEBNext® Microbiome DNA Enrichment Kit, NEB). Following this, both sets of samples were used to prepare libraries using the KAPA LTP kit (Roche) with unique dual indices (NEBNext® Multiplex oligos for Illumina, NEB). The resulting libraries were pooled in equimolar amounts and sequenced using a NextSeq500 (Illumina) to obtain paired end reads using 150X150 cycles.

Target enrichment sequencing

Following on the library preparation step described above, DNA and RNA derived libraries were pooled separately and were incubated with the VirCapSeq-VERT Capture Panel probes (Roche) following the manufacturer's guidelines. The Roche VirCapSeq-VERT Capture Panel covers the genomes of 207 viral taxa known to infect vertebrates (including humans). Enriched DNA and RNA- derived libraries were further amplified using 14 PCR cycles, pooled and sequenced using a NextSeq500 (Illumina) to obtain paired end reads using 150X150 cycles.

Bioinformatics analysis

Reads for each sample were first quality checked, Illumina adapters were trimmed using Trim Galore (https://github.com/FelixKrueger/TrimGalore) and then mapped to the human genome using BWA-MEM (https://github.com/lh3/bwa). Only reads that did not map to the human genome were used for metagenomic analyses. Reads per million were calculated as the number of viral reads per million reads sequenced, to normalise for variation in sample sequencing depth. Non-human reads were then *de novo* assembled using MetaSPAdes (https://github.com/ablab/spades) to generate contigs for each sample. Contigs were compared against a protein database of all NCBI RefSeq organisms (including virus, bacteria, eUnited Kingdomaryotes) with BLASTX using DIAMOND (https://github.com/bbuchfink/diamond). In addition, non-human reads for each sample were aligned to a small panel of HAdV NCBI RefSeq genomes (HAdV-A, B1, B2, C, D, E, F, 1, 2, 5, 7, 35, 54 as well as HAdV-F41).

The nine AAV2 near-complete genome contigs from the plasma samples were assembled and compared with sequences in GenBank using BLASTN (nucleotide database). Each of these AAV2 genomes had numerous close hits (exhibiting >95% similarity across 95% of the genome) with various existing AAV2 sequences; those most closely related were reported in a recent publication[31] All linear complete AAV2 genomes returned via BLAST against the GenBank nt database with a query coverage >75%, were selected and combined with the AAV sequences *de novo* assembled here and aligned with MAFFT. The terminal ends of this alignment were trimmed off and IQ-TREE 2 was used (TIM+F+R3 model) to infer a phylogenetic tree. For the single HAdV41 genome *de novo* assembled, all available HAdV41 complete genomes were downloaded from GenBank, aligned with MAFFT and IQ-TREE2 was used (K2P+R2 model) to infer a phylogenetic tree.

Anti-AAV2 ELISA Assay

AAV2 pAAV-CAG-tdTomato viral preparation (codon diversified) was a gift from Edward Boyden (Addgene viral prep #59462-AAV2; http://n2t.net/addgene:59462; RRID:Addgene_59462).

AAV2 particles, obtained from Addgene (cat. No. 59462-AAV2, Addgene, United Kingdom), were diluted in PBS and used to coat a Immulon 2HB 96-well flat bottom plate (ImmunoChemistry Technologies, LLC, CA, USA) at a concentration of $1x10^8$ particles per well. The plates were incubated on an orbital shaker overnight at 4^0C. Plates were then blocked with PBS-T (PBS, 0.1% Tween20) containing 5% BSA for 1 hour prior to the addition on samples. The plates were washed five times in PBS-T before serum samples, diluted 1:50 in PBS, were added in triplicate. A mouse anti-AAV2 (A20, Progen, Germany) was used as a positive control at a concentration of 1:50. Samples were incubated at room temperature on an orbital shaker for 1:30 hrs before washing five times in PBS-T and adding either Anti-Human IgM or Anti-Human IgG (Merck, United Kingdom cat no. A9794 and A1543, respectively) diluted 1:10000, Goat Anti-Mouse IgG (Merck, United Kingdom cat no. A2429) was used as the secondary for the anti AAV2 A20 positive control. The plates were incubated for 1hr before washing five times with PBS-T then 100ul of Alkaline Phosphatase yellow (Merck, United Kingdom cat no. P7998) was added an incubated for 15 minutes before stopping the reaction with 3M NaOH and measuring absorbance at 405nm.

Immunohistochemistry, in situ-hybridization, and special staining

Formalin-fixed and paraffin-wax embedded liver samples were cut at ~3 micrometre thickness and mounted on glass slides. A reticulin (1936) and Masson trichrome (1929) special staining

(Gordon and Sweets method (1936)) was performed. Antibodies used for immunohistochemistry are listed in Supplementary Table 6.

Detection of viral nucleic acids as well as ubiquitin and DapB-specific RNA (Advanced Cell Diagnostics, AAV2 (1195791), HHV6 (144565), Adenovirus 41 (1192351, Ubiquitin (310041) and DapB (310043)) was performed following the manufacturer's protocol with pretreatment with simmering in target solution (30 min) and additional proteinase K (30 min.) treatment. A haematoxylin counterstain was performed, and slides were mounted with Vectamount mounting media (# H-500, Vector Laboratories) and scanned with a bright field slide scanner (Leica, Aperio Versa 8).

Liver histopathology grading

Liver scoring was performed as previously described[8,9].

Quantification of immune cells

After scanning of the whole slides, liver tissue was outlined and the number of positively stained cells (DAB signal for immunohistochemistry or Fast Red signal for *in situ*-hybridization) was assessed using software assisted image analysis (QuPath version 0.3.2)[34]. For each marker, the cell detection algorithm was tuned, and data plotted in Graph Pad Prism (version 9.4.1).

Spatial analysis (Codex Phenocycler)

Formalin fixed, paraffin-wax embedded liver samples (patient 228742A and 145808) were sectioned at 2 to 4 micrometre thickness on 22 mm x 22 mm glass coverslips (Akoya Biosciences, #7000005) coated in 0.1% poly-L-lysine (Sigma-Aldrich, Cat. P8920). Antigen retrieval was performed by pressure cooking with citrate buffer at pH 6. Carrier-free, pre-

conjugated antibodies were purchased directly from Akoya Biosciences or purchased from other suppliers in preparation for custom-conjugation**.** If carrier-free antibodies were not available, alternatives were purchased and purified using a Pierce^{TM} antibody cleanup kit (Ref #44600, Thermofisher). Antibodies were custom conjugated to a unique oligonucleotide barcode according to manufacturer's instructions using an antibody conjugation kit (Ref #7000009, Akoya Biosciences) and stored at 4°C for at least 48 hours before use. Conjugated antibodies were stored at 4°C.

Coverslips with tissue were rehydrated in an alcohol series and washed in distilled water, before performing heat-induced antigen retrieval in a pressure cooker with citrate buffer (pH 6). Glass coverslips were then moved progressively between wells of a 6-well plate containing components of the CODEX staining kit (Akoya Biosciences, #7000008). This included 2 wells of hydration buffer (2 mins each), 1 well of staining buffer (20 mins), and then staining with 190ul of an 11-marker antibody panel **(**Supplementary Table 7**)**. Tissue sections of both samples were treated in the same way on the same day and were incubated with antibodies for 3 hours at room temperature (RT) simultaneously. Following staining, tissue was incubated twice in staining buffer (2 min each) and transferred to a post-staining fixation solution made from a 1:10 ratio of PFA:storage buffer fo r 10 mins. Tissues were then washed 3 times in 1X phosphate buffered saline (PBS; #14190-094, Gibco), incubated in ice-cold methanol (# M/4000/PC17, Fisher scientific) for 5 mins on ice, and again washed 3 times in PBS. Tissue sections were fixed in a fixative solution for 20 mins, washed 3x in PBS and stored in storage buffer until image acquisition

Image acquisition was achieved using a Keyence BZ-X710 microscope equipped with 4 fluorescent channels (one nuclear stain, 3 for antibody visualization). In a 96-well plate (Akoya Biosciences, #7000006), a maximum of three oligonucleotide reporters are used per well

(cycle) (5 microlitre each) and added to between 235 microlitre -245microlitre reporter stock solution created according to manufacturer's instructions. Plates were sealed with aluminum film (Akoya Biosciences, #7000007) and stored at 4°C until use. Pictures were captured with QuPath version 0.3.2 https://www.nature.com/articles/s41598-017-17204-5.

Host genetics and HLA typing

High resolution typing for all HLA loci (HLA-A, B, C, DRB1, DRB3/4/5, DQA1, DQB1, DPA1 and DPB1) was performed using AllType™ FASTplex™ NGS Assay (One Lambda) run on an Illumina Mi-Seq platform. HLA typing was undertaken on 27 ISARIC consented patients. One patient was omitted from analysis as they were a sibling of another case. HLA types from 64 Scottish National Blood Transfusion Service apheresis platelet donors, self-identified as White British (n=15) or White Scottish (n=49) were used as control samples for comparison with patient HLA allele frequencies. Genotyping was performed using the Illumina Global Screening Array v3.0 + multi-disease beadchips (GSAMD-24v3-0-EA) and Infinium chemistry. This consists of three steps: (1) whole genome amplification, (2) fragmentation followed by hybridisation, and (3) single-base extension and staining. Arrays were imaged on an Illumina iScan platform and genotypes were called automatically using GenomeStudio Analysis software v2.0.3, GSAMD-24v3-0-EA_20034606_A1.bpm manifest and cluster file provided by manufacturer.

Given the small sample size, it was not possible to implement quality control processes using GenomeStudio and manufacturer's published recommendations. As genotyping was conducted using the same genotyping array used for the genOMICC study, variants that passed quality control for the genOMICC study were retained, as described previously[35]. After further

excluding variants with call rates <95%, a total of 478,692 variants was used for downstream analysis.

Kinship and population structure

To identify close relatives up to 3rd degree King 2.1 was used, confirming the presence of a pair of siblings with no further close relatives identified. Genotypes of 19 patients were combined with imputed genotypes of a subset of unrelated United Kingdom Biobank participants obtained by removing one individual in each pair with estimated kinship larger than 0.0442. The resulting genotypes were filtered to exclude variants with MAF < 5%, genotype missingness rate < 1.5%, and Hardy–Weinberg equilibrium (HWE) $P < 10^{-50}$. Principal component analysis (PCA) was conducted with gcta 1.955 in the set of unrelated individuals with pruned SNPs using a window of 1,000 markers, a step size of 50 markers and an r2 threshold of 0.01. Analyses were performed once including all United Kingdom Biobank participants and once including only United Kingdom Biobank participants who were born in Scotland (United KingdomB Field 1647) and of Caucasian genetic ancestry (United KingdomB Field 22006).

Statistics

Differences between cases and control groups were tested using Fisher's Exact Test for categorical variables and Mann-Whitney (two tailed) for continuous variables respectively using R studio version 1.2.5033, R version 4.1.2 and GraphPad version 9.0.0.

For coronavirus serology experiments, comparisons were carried out with one way ANOVA and TUnited Kingdomey's Multiple Comparison test, carried out in GraphPad version 8.4.3.

HLA analysis used the Bridging ImmunoGenomic Data-Analysis Workflow Gaps (BIGDAWG) R package to derive OR and corrected p values for individual HLA alleles[36]. Bonferroni corrected p value significance threshold, adjusted for multiple comparisons (168 HLA alleles), was $p<3.0\times10^{-4}$.

Figures

Figures were prepared using Microsoft Office Excel 2010, Microsoft Office Powerpoint 2010 and Adobe Illustrator 2022.

Reporting summary

Further information on research design is available in the Nature Research Reporting Summary linked to this paper.

Data availability

Datasets generated in the current study are appended as Source Data and Supplementary Tables. Data, protocols, and all documentation around this analysis may be made available to academic researchers after authorisation from the independent data access and sharing committee. Clinical data and analysis scripts are available on request to the Independent Data Management and Access Committee at https://isaric4c.net/ sample_access. Restrictions apply to the availability of identifiable clinical data. Due to the relatively small number of cases, de-aggregation of data is potentially disclosive, as is the patient-level line list data. Therefore, a formal data sharing agreement is required for data access. The Independent Data and Material Access Committee considers requests as they arrive; most responses are made within 28 days. Use of clinical samples are also restricted under ethical approvals obtained for their use. Genome sequences are available in GenBank with accession numbers for AAV2: OP019741-OP019749 and for HAdV-F41: OP019750.

Code availability

Freely available bioinformatics and statistical software were used, see links in the Methods section.

References

1 Marsh, K. *et al.* Investigation into cases of hepatitis of unknown aetiology among young children, Scotland, 1 January 2022 to 12 April 2022. *Euro Surveill* **27**, doi:10.2807/1560-7917.ES.2022.27.15.2200318 (2022).

2 World Health Organization. *Severe acute hepatitis of unknown aetiology in children - Multi-country*, <https://www.who.int/emergencies/disease-outbreak-news/item/2022-DON400> (2022).

3 United Kingdom Health Security Agency. Investigation into acute hepatitis of unknown aetiology in children in England - Technical Briefing 4. (United KingdomHSA, 2022).

4 Gutierrez Sanchez, L. H. *et al.* A Case Series of Children with Acute Hepatitis and Human Adenovirus Infection. *N Engl J Med*, doi:10.1056/NEJMoa2206294 (2022).

5 Karpen, S. J. Acute Hepatitis in Children in 2022 - Human Adenovirus 41? *N Engl J Med*, doi:10.1056/NEJMe2208409 (2022).

6 Kelgeri, C. *et al.* Clinical Spectrum of Children with Acute Hepatitis of Unknown Cause. *N Engl J Med*, doi:10.1056/NEJMoa2206704 (2022).

7 Dunning, J. W. *et al.* Open source clinical science for emerging infections. *Lancet Infect Dis* **14**, 8-9, doi:10.1016/S1473-3099(13)70327-X (2014).

8 Knodell, R. G. *et al.* Formulation and application of a numerical scoring system for assessing histological activity in asymptomatic chronic active hepatitis. *Hepatology* **1**, 431-435, doi:10.1002/hep.1840010511 (1981).

9 Krishna, M. Histological Grading and Staging of Chronic Hepatitis. *Clin Liver Dis (Hoboken)* **17**, 222-226, doi:10.1002/cld.1014 (2021).

10 Public Health Scotland. *Enhanced Surveillance of Covid-19 in Scotland (Population-based seroprevalence) - 5 week rolling estimate.*, <https://publichealthscotland.scot/publications/enhanced-surveillance-of-covid-19-in-scotland/enhanced-surveillance-of-covid-19-in-scotland-population-based-seroprevalence-surveillance-1-june-2022/dashboard/> (2022).

11 Rodriguez-Inigo, E. *et al.* Percentage of hepatitis C virus-infected hepatocytes is a better predictor of response than serum viremia levels. *J Mol Diagn* **7**, 535-543, doi:10.1016/S1525-1578(10)60585-5 (2005).

12 Tomlinson, J. E. *et al.* Tropism, pathology, and transmission of equine parvovirus-hepatitis. *Emerg Microbes Infect* **9**, 651-663, doi:10.1080/22221751.2020.1741326 (2020).

13 Leen, G., Stein, J. E., Robinson, J., Maldonado Torres, H. & Marsh, S. G. E. The HLA diversity of the Anthony Nolan register. *HLA* **97**, 15-29, doi:10.1111/tan.14127 (2021).

14 Srivastava, A., Lusby, E. W. & Berns, K. I. Nucleotide sequence and organization of the adeno-associated virus 2 genome. *J Virol* **45**, 555-564, doi:10.1128/JVI.45.2.555-564.1983 (1983).

15 Atchison, R. W., Casto, B. C. & Hammon, W. M. Adenovirus-Associated Defective Virus Particles. *Science* **149**, 754-756, doi:10.1126/science.149.3685.754 (1965).

16 Li, C. *et al.* Neutralizing antibodies against adeno-associated virus examined prospectively in pediatric patients with hemophilia. *Gene Ther* **19**, 288-294, doi:10.1038/gt.2011.90 (2012).

17 Martino, A. T. *et al.* Engineered AAV vector minimizes in vivo targeting of transduced hepatocytes by capsid-specific CD8+ T cells. *Blood* **121**, 2224-2233, doi:10.1182/blood-2012-10-460733 (2013).

18 Manno, C. S. *et al.* Successful transduction of liver in hemophilia by AAV-Factor IX and limitations imposed by the host immune response. *Nat Med* **12**, 342-347, doi:10.1038/nm1358 (2006).

19 Mingozzi, F. *et al.* CD8(+) T-cell responses to adeno-associated virus capsid in humans. *Nat Med* **13**, 419-422, doi:10.1038/nm1549 (2007).

20 Ertl, H. C. J. Immunogenicity and toxicity of AAV gene therapy. *Front Immunol* **13**, 975803, doi:10.3389/fimmu.2022.975803 (2022).

21 Chowdary, P. *et al.* Phase 1-2 Trial of AAVS3 Gene Therapy in Patients with Hemophilia B. *N Engl J Med* **387**, 237-247, doi:10.1056/NEJMoa2119913 (2022).

22 Sebode, M., Weiler-Normann, C., Liwinski, T. & Schramm, C. Autoantibodies in Autoimmune Liver Disease-Clinical and Diagnostic Relevance. *Front Immunol* **9**, 609, doi:10.3389/fimmu.2018.00609 (2018).

23 Rafie, K. *et al.* The structure of enteric human adenovirus 41-A leading cause of diarrhea in children. *Sci Adv* **7**, doi:10.1126/sciadv.abe0974 (2021).

24 Echavarria, M. Adenoviruses in immunocompromised hosts. *Clin Microbiol Rev* **21**, 704-715, doi:10.1128/CMR.00052-07 (2008).

25 Baker, J. M. *et al.* Acute Hepatitis and Adenovirus Infection Among Children - Alabama, October 2021-February 2022. *MMWR Morb Mortal Wkly Rep* **71**, 638-640, doi:10.15585/mmwr.mm7118e1 (2022).

26 Cooper, S. *et al.* Long COVID-19 Liver Manifestation in Children. *J Pediatr Gastroenterol Nutr*, doi:10.1097/MPG.0000000000003521 (2022).

27 Deep, A., Grammatikopoulos, T., Heaton, N., Verma, A. & Dhawan, A. Outbreak of hepatitis in children: clinical course of children with acute liver failure admitted to the intensive care unit. *Intensive Care Med*, doi:10.1007/s00134-022-06765-3 (2022).

28 van Gerven, N. M. *et al.* HLA-DRB1*03:01 and HLA-DRB1*04:01 modify the presentation and outcome in autoimmune hepatitis type-1. *Genes Immun* **16**, 247-252, doi:10.1038/gene.2014.82 (2015).

29 Lanchbury, J. S. *et al.* Strong primary selection for the Dw4 subtype of DR4 accounts for the HLA-DQw7 association with Felty's syndrome. *Hum Immunol* **32**, 56-64, doi:10.1016/0198-8859(91)90117-r (1991).

30 Gay, D. *et al.* Functional interaction between human T-cell protein CD4 and the major histocompatibility complex HLA-DR antigen. *Nature* **328**, 626-629, doi:10.1038/328626a0 (1987).

31 La Bella, T. *et al.* Adeno-associated virus in the liver: natural history and consequences in tumour development. *Gut* **69**, 737-747, doi:10.1136/gutjnl-2019-318281 (2020).

Methods References

32 Aurnhammer, C. *et al.* Universal real-time PCR for the detection and quantification of adeno-associated virus serotype 2-derived inverted terminal repeat sequences. *Hum Gene Ther Methods* **23**, 18-28, doi:10.1089/hgtb.2011.034 (2012).

33 Gautheret-Dejean, A. *et al.* Development of a real-time polymerase chain reaction assay for the diagnosis of human herpesvirus-6 infection and application to bone marrow transplant patients. *J Virol Methods* **100**, 27-35, doi:10.1016/s0166-0934(01)00390-1 (2002).

34 Bankhead, P. *et al.* QuPath: Open source software for digital pathology image analysis. *Sci Rep* **7**, 16878, doi:10.1038/s41598-017-17204-5 (2017).

35 Pairo-Castineira, E. *et al.* Genetic mechanisms of critical illness in COVID-19. *Nature* **591**, 92-98, doi:10.1038/s41586-020-03065-y (2021).

36 Pappas, D. J., Marin, W., Hollenbach, J. A. & Mack, S. J. Bridging ImmunoGenomic Data Analysis Workflow Gaps (BIGDAWG): An integrated case-control analysis pipeline. *Hum Immunol* **77**, 283-287, doi:10.1016/j.humimm.2015.12.006 (2016).

Acknowledgements We wish to acknowledge the contribution of the participating children and their parents who agreed to participate in the ISARIC CCP-United Kingdom and DIAMONDS studies, and the research teams who recruited the patients. The work was funded by Public Health Scotland, the National Institute for Health Research (NIHR; award CO-CIN-01) and the Medical Research Council (MRC; grants MR/X010252/1, MC_UU_1201412, MC_UU_12018/12, MC_PC_19059, MC_PC_19025 & MC_PC_22004). DIAMONDS is funded by the European Union Horizon 2020 programme; grant 848196). MP acknowledges funding support from the Wellcome Trust (206369/Z/17/Z). MGS gratefully acknowledges funding support from The Pandemic Institute, Liverpool and the NIHR Health Protection Research Unit (HPRU) in Emerging and Zoonotic Infections at University of Liverpool, and United Kingdom Health Security Agency (United KingdomHSA). JKB gratefully acknowledges funding support from a Wellcome Trust Senior Research Fellowship (223164/Z/21/Z), and MC_PC_20029, Sepsis Research (Fiona Elizabeth Agnew Trust), a BBSRC Institute Strategic Programme Grant to the Roslin Institute (BB/P013732/1, BB/P013759/1), and the United Kingdom Intensive Care Society. We gratefully acknowledge the support of Baillie Gifford and the Baillie Gifford Science Pandemic Hub at the University of Edinburgh. Parts of this research has been conducted using the United Kingdom Biobank Resource under project 788 and we would like to acknowledge the assistance of Prof. Albert Tenesa in making this possible. Additional replication was also conducted using the United Kingdom Biobank Resource (Project 26041).We also acknowledge the support of NHS Research Scotland (NRS) Greater Glasgow and Clyde Biorepository team. We thank Susan Bennett-Slater from NHS Greater Glasgow and Clyde for assisting with sample location and testing. The authors would like to thank the histopathology team, Veterinary Diagnostic, University of Glasgow, for excellent technical assistance. We acknowledge Pablo Murcia for providing resources and advice and Paula Olmo for administrative assistance. Lastly, we

acknowledge the invaluable advice of Eric J. Kremer from the Institut de Génétique Moléculaire de Montpellier, Université de Montpellier and Andrew Baker, University of Edinburgh. For the purpose of open access, the author has applied a CC BY public copyright licence to any Author Accepted Manuscript version arising from this submission.

Author contributions AH, AdSF, JKB, ECT conceived the study. AH, RO, DLR, PA, VH, CD, BW, DT, RB, NA, JKB, JH, PH, SR, CW and ECT did the formal analysis. AH, RT, PA, VH, CD, LT, KS, MM, JA, BW, KR, LP, LG, CE, JM, KR, KM, TD, MTGH, ML, DY, SC, MO'L, MP, DH, AM, NM, AdSF, JB, DT, RB, PH, MO, PC, WO, MC and ECT did the investigation. SEM, EV, TD, SS, CJ, RG, AM, NM, AB-S, MSH, DE-R, MGS, ML provided resources. NA, EP-C and VV performed validation. AH and ECT wrote the original draft of the manuscript. AH, RO, RT, PA, LP, JM, KR, KM, TD, MH, ML, PH, MC, ML, MP, DLR, AdSF, BW, JB, MGS, DT, JKB and ECT reviewed and edited the manuscript. RO, PA, VH, CD, KR, BW and ECT visualised the data.

Competing interests The authors declare no competing interests.
Additional information
Supplementary information is available for this paper at
Correspondence and requests for materials should be addressed to Emma C Thomson.
Peer review information *Nature* thanks Leif Sander, Frank Tacke and the other, anonymous, reviewer(s) for their contribution to the peer review of this work. Peer reviewer reports are available.
Reprints and permissions information is available at www.nature.com/reprints.

DIAMONDS Consortium

Michael Levin[13], Aubrey Cunnington[13], Jethro Herberg[13], Myrsini Kaforou[13], Victoria Wright[13], Evangelos Bellos[13], Claire Broderick[13], Samuel Channon-Wells[13], Samantha Cooray[13], Tisham De[13], Giselle D'Souza[13], Leire Estramiana Elorrieta[13], Diego Estrada-Rivadeneyra[13], Rachel Galassini[13], Dominic Habgood-Coote[13], Shea Hamilton[13], Heather Jackson[13], James Kavanagh[13], Mahdi Moradi Marjaneh[13],

Stephanie Menikou[13], Samuel Nichols[13], Ruud Nijman[13], Harsita Patel[13], Ivana Pennisi[13], Oliver Powell[13], Ruth Reid[13], Priyen Shah[13], Ortensia Vito[13], Elizabeth Whittaker[13], Clare Wilson[13], Rebecca Womersley[13], Amina Abdulla[19], Sarah Darnell[19], Sobia Mustafa[19], Pantelis Georgiou[20], Jesus-Rodriguez Manzano[21], Nicolas Moser[20], Ivana Pennisi[3], Michael Carter[22,23] , Shane Tibby[22,23], Jonathan Cohen[22], Francesca Davis[22], Julia Kenny[22], Paul Wellman[22], Marie White[22], Matthew Fish[24], Aislinn Jennings[25], Manu Shankar-Hari[24,25], Katy Fidler[26] , Dan Agranoff[27], Vivien Richmond[26,28], Mathew Seal[27], Saul Faust[29] , Dan Owen[29], Ruth Ensom[30], Sarah McKay[30], Diana Mondo[31], Mariya Shaji[31], Rachel Schranz[31], Prita Rughnani[32,33,34,] Amutha Anpananthar[32,33,34], Susan Liebeschuetz[33], Anna Riddell[32], Nosheen Khalid[32],[34], Ivone Lancoma Malcolm[34], Teresa Simagan[34], Mark Peters[35],[36] , Alasdair Bamford[35],[36], Lauran O'Neill[35], Nazima Pathan[37],[38], Esther Daubney[37], Deborah White[37], Melissa Heightman[39] , Sarah Eisen[39] (,), Terry Segal[39], Lucy Wellings[39] , Simon B Drysdale[40] , Nicole Branch[40], Lisa Hamzah[40], Heather Jarman[40] Maggie Nyirenda[41], [3], , Lisa Capozzi[41], Emma Gardiner[41] Robert Moots[42] , Magda Nasher[42], Anita Hanson[43], Michelle Linforth[42] Sean O'Riordan[44], Donna Ellis[44] Akash Deep[45], Ivan Caro[45] Fiona Shackley[46], Arianna Bellini[46], Stuart Gormley[46] Samira Neshat[47] Barnaby J Scholefield[48], Ceri Robbins[48], Helen Winmill[48] , Stéphane C. Paulus[49,50,51], Andrew J. Pollard[49,50,51,52], Mark Anthony[49], Sarah Hopton[49], Danielle Miller[49], Zoe Oliver[49], Sally Beer[49], Bryony Ward[49] , Shrijana Shrestha[53],Andrew J Pollard[54],[55], Meeru Gurung[53], Puja Amatya[53], Bhishma Pokhrel[53], Sanjeev Man BijUnited Kingdomchhe[53], Tim Lubinda[54], Sarah Kelly[54], Peter O'Reilly[54] , Federico Martinón-Torres[56], Antonio Salas[56],[57] Fernando Álvez González[56], Xabier Bello[56],[58], Mirian Ben García[56], Sandra Carnota[56], Miriam Cebey-López[56], María José Curras-Tuala[56],[57], Carlos Durán Suárez[56], Luisa García Vicente[56], Alberto Gómez-Carballa[56],[57] Jose Gómez Rial[56], Pilar Leboráns Iglesias[56], Federico Martinón-Torres[56], Nazareth Martinón-Torres[56], José María Martinón Sánchez[56], Belén Mosquera Pérez[56],

Jacobo Pardo-Seco[56,57], Lidia Piñeiro Rodríguez[56], Sara Pischedda[56,57] Sara Rey Vázquez[56], Irene Rivero Calle[56], Carmen Rodríguez-Tenreiro[56], Lorenzo Redondo-Collazo[56], Miguel Sadiki Ora[56], Antonio Salas[56,57] Sonia Serén Fernández[56], Cristina Serén Trasorras[56], Marisol Vilas Iglesias[56] , Enitan D Carrol[59,60], Elizabeth Cocklin[59], Aakash Khanijau[59], Rebecca Lenihan[59], Nadia Lewis-Burke[59], Karen Newall[60], Sam Romaine[59], Maria Tsolia[61], Irini Eleftheriou[61], Nikos Spyridis[61], Maria Tambouratzi[61], Despoina Maritsi[61], Antonios Marmarinos[61], Marietta Xagorari[61], Lourida Panagiota[62], Pefanis Aggelos[62], Akinosoglou Karolina[63], Gogos Charalambos[63], Maragos Markos[63], Voulgarelis Michalis[64], Stergiou Ioanna[64], Marieke Emonts [65,66,67], Emma Lim[66,67,70], John Isaacs[65] , Kathryn Bell[68], Stephen Crulley[68], Daniel Fabian[68], Evelyn Thomson[68], Diane Wallia[68], Caroline Miller[68], Ashley Bell[68], Fabian J.S. van der Velden[65,66] , , Geoff Shenton[71], Ashley Price[72,73],Owen Treloar [65,66], Daisy Thomas[65,66], Pablo Rojo[74,76], Cristina Epalza[74,75], Serena Villaverde[74], Sonia Márquez[75], Manuel Gijón[75], Fátima Machín[75], Laura Cabello[75], Irene Hernández[75], Lourdes Gutiérrez[75], Ángela Manzanares[74], T.W. (Taco) Kuijpers MD PhD[77,78] , M. (Martijn) van de Kuip MD PhD[77], A.M. (Marceline) van Furth MD PhD[77], J.M. (Merlijn) van den Berg MD PhD[77], Giske Biesbroek MD PhD[77], Floris Verkuil MD [77], Carlijn (C.W.) van der Zee MD[77], Dasja Pajkrt MD PhD[77], Michael Boele van Hensbroek MD PhD[77], Dieneke Schonenberg MD[77], Mariken Gruppen MD[77], Sietse Nagelkerke MD PhD[77,78], Machiel H Jansen[77], Ines Goetschalckx[78], Lorenza Romani[79] , Maia De Luca[79], Sara Chiurchiù[79], Martina Di Giuseppe[79], Clementien L. Vermont[81], Henriëtte A. Moll[80], Dorine M. Borensztajn[80], Nienke N. Hagedoorn[80], Chantal Tan[80], Joany Zachariasse[80], Medical students[80], W Dik[82], Ching-Fen (Kitty), Shen[83], Dace Zavadska[84,85], Sniedze Laivacuma[84,86], Aleksandra Rudzate[84,85], Diana Stoldere[84,85], Arta Barzdina[84,85], Elza Barzdina[84,85], Sniedze Laivacuma[84,86], Monta Madelane[84,86], Dagne Gravele[85], Dace Svile[85], Romain Basmaci[87,88], Noémie Lachaume[87], Pauline Bories[87], Raja Ben Tkhayat[87], Laura Chériaux[87], Juraté Davoust[87], Kim-Thanh Ong[87],

Marie Cotillon[87], Thibault de Groc[87], Sébastien Le[87], Nathalie Vergnault[87], Hélène Sée[87], Laure Cohen[87], Alice de Tugny[87], Nevena Danekova[87], Marine Mommert-Tripon[89], Karen Brengel-Pesce[89], Marko Pokorn[90],[91],[92], Mojca Kolnik[91], Tadej Avčin[91],[92], Tanja Avramoska[91], Natalija Bahovec[90], Petra Bogovič[90], Lidija Kitanovski[91],[92], Mirijam Nahtigal[90], Lea Papst[90], Tina Plankar Srovin[90], Franc Strle[90],[91], Anja Srpčič[91], Katarina Vincek[90], Michiel van der Flier[94],[98] , Wim J.E. Tissing[95], Roelie M. Wösten-van Asperen[95], Sebastiaan J Vastert[96], Daniel C Vijlbrief[97], Louis J. Bont[94],[98] , Tom F.W. Wolfs[94],[98] , Coco R. Beudeker[94],[98] , Philipp Agyeman[99], Luregn Schlapbach[100],[101], Christoph Aebi[99], Mariama Usman[99], Stefanie Schlüchter[99], Verena Wyss[99], Nina Schöbi[99], Elisa Zimmermann[100], Marion Meier[100], Kathrin Weber[100], Philipp Agyeman, MD[102], Luregn J Schlapbach MD, FCICM[103],[104], Eric Giannoni, MD[105],[106], Martin Stocker, MD[107], Klara M Posfay-Barbe, MD[108], Ulrich Heininger, MD[109], Sara Bernhard-Stirnemann, MD[110], Anita Niederer-Loher, MD[111], Christian Kahlert, MD[111], Giancarlo Natalucci, MD[112], Christa Relly, MD[113], Thomas Riedel, MD[114], Christoph Aebi, MD[102], Christoph Berger, MD[113], Prof Colin Fink[115], Marie Voice[115], Leo Calvo-Bado[115], Michael Steele[115], Jennifer Holden[115], Benjamin Evans[115], Jake Stevens[115], Peter Matthews[115], Kyle Billing[115], Werner Zenz[116], Alexander Binder[116], Benno Kohlmaier[116], Daniela S. Kohlfürst[116], Nina A. Schweintzger[116] , , Christoph Zurl[116], Susanne Hösele[116], Manuel Leitner[116], Lena Pölz[116], Alexandra Rusu[117], Glorija Rajic[116], Bianca Stoiser[116], Martina Strempfl[116], Manfred G. Sagmeister[116], Sebastian Bauchinger[116], Martin Benesch[118], Astrid Ceolotto[116], Ernst Eber[117], Siegfried Gallistl[116], Harald Haidl[116], Almuthe Hauer[116], Christa Hude[116], Andreas Kapper[119], Markus Keldorfer[120], Sabine Löffler[120], Tobias Niedrist[121], Heidemarie Pilch[120], Andreas Pfleger[117], Klaus Pfurtscheller[119], Siegfried Rödl[119], Andrea Skrabl-Baumgartner[116], Volker Strenger[118], Elmar Wallner[122], Dennie Tempel[123], Danielle van Keulen[123], Annelieke M Strijbosch[123], Maike K. Tauchert[124], Ulrich von Both[125],[126] MD, FRCPCH , Laura Kolberg[125]

MSc , Patricia Schmied[125], Irene Alba-Alejandre[127], **Katharina Danhauser, MD[130]**, **Nikolaus Haas, MD[135]**, **Florian Hoffmann, MD[134],** Matthias Griese, MD[131], Tobias Feuchtinger, MD[129], Sabrina Juranek, MD[128], Matthias Kappler, MD[131], Eberhard Lurz, MD[132], **Esther Maier, MD[128]**, Karl Reiter, MD[134], Carola Schoen, MD[134], **Sebastian Schroepf[133]**, Shunmay Yeung [18],[136], Manuel Dewez[18], David Bath[137], Elizabeth Fitchett[18], Fiona Cresswell[18]

19. Children's Clinical Research Unit, St Mary's Hospital, Praed Street, London W2 1NY, United Kingdom

20. Imperial College London, Department of Electrical and Electronic Engineering, South Kensington Campus, London, SW7 2AZ, United Kingdom

21. Imperial College London, Department of Infectious Disease, Section of Adult Infectious Disease, Hammersmith Campus, London, W12 0NN, United Kingdom

22. Evelina London Children's Hospital, Guy's and St Thomas' NHS Foundation Trust, London, United Kingdom

23. Department of Women and Children's Health, School of Life Course Sciences, King's College London, United Kingdom

24. Department of Infectious Diseases, School of Immunology and Microbial Sciences, King's College London, London, United Kingdom

25. Department of Intensive Care Medicine, Guy's and St Thomas' NHS Foundation Trust, London, United Kingdom

26. Royal Alexandra Children's Hospital, University Hospitals Sussex, Brighton, United Kingdom

27. Dept of Infectious Diseases, University Hospitals Sussex, Brighton, United Kingdom

28. Research Nurse team, University Hospitals Sussex, Brighton, United Kingdom

29. NIHR Southampton Clinical Research Facility, University Hospital Southampton NHS Foundation Trust and University of Southampton, United Kingdom

30. NIHR Southampton Clinical Research Facility, University Hospital Southampton NHS Foundation Trust, United Kingdom

31. Department of R&D, University Hospital Southampton NHS Foundation Trust, United Kingdom

32. Royal London Hospital, Whitechapel Rd, London E1 1FR, United Kingdom

33. Newham University Hospital, Glen Rd, London E13 8SL, United Kingdom

34. Whipps Cross University Hospital, Whipps Cross Road, London, E11 1NR, United Kingdom

35. Great Ormond Street Hospital, London, WC1N 3JH, United Kingdom

36. UCL Great Ormond St Institute of Child Health, WC1N 1EH, United Kingdom

37. Addenbrooke's Hospital, Hills Road, Cambridge CB2 0QQ, United Kingdom

38. Department of Paediatrics, University of Cambridge, Cambridge CB2 0QQ, United Kingdom

39. University College London Hospital, Euston Road, London NW1 2BU, United Kingdom

40. St George's Hospital, Blackshaw Road, London SW17 0QT, United Kingdom

41. University Hospital Lewisham, London SE13 6LH, United Kingdom

42. Aintree University Hospital, Lower Lane, Liverpool L9 7AL, United Kingdom

43. Royal Liverpool Hospital, Prescot St, Liverpool L7 8XP, United Kingdom

44. Leeds Children's Hospital, Leeds LS1 3EX, United Kingdom

45. Kings College Hospital, Denmark Hill, London SE5 9RS, United Kingdom

46. Sheffield Children's Hospital, Broomhall, Sheffield S10 2TH, United Kingdom

47. Leicester General Hospital, Leicester LE1 5WW, United Kingdom

48. Birmingham Children's Hospital, Steelhouse Lane, Birmingham B4 6NH, United Kingdom

49. John Radcliffe Hospital, Oxford University Hospitals NHS Foundation Trust, Oxford, United Kingdom

50. Department of Paediatrics, University of Oxford, United Kingdom

51. Oxford Vaccine Group, University of Oxford, United Kingdom

52. NIHR Oxford Biomedical Research Centre, Oxford, United Kingdom

53. Paediatric Research Unit, Patan Academy of Health Sciences, Kathmandu, Nepal.

54. Oxford Vaccine Group, Department of Paediatrics, University of Oxford, Oxford, United Kingdom

55. NIHR Oxford Biomedical Research Centre, Oxford, United Kingdom

56. Translational Pediatrics and Infectious Diseases, Pediatrics Department, Hospital Clínico Universitario de Santiago, Santiago de Compostela, Spain, and GENVIP Research Group (www.genvip.org), Instituto de Investigación Sanitaria de Santiago, Universidad de Santiago de Compostela, Galicia, Spain.

57. Unidade de Xenética, Departamento de Anatomía Patolóxica e Ciencias Forenses, Instituto de Ciencias Forenses, Facultade de Medicina, Universidade de Santiago de Compostela, and GenPop Research Group, Instituto de Investigaciones Sanitarias (IDIS), Hospital Clínico Universitario de Santiago, Galicia, Spain

58. Fundación Pública Galega de Medicina Xenómica, Servizo Galego de Saúde (SERGAS), Instituto de Investigaciones Sanitarias (IDIS), and Grupo de Medicina Xenómica, Centro de Investigación Biomédica en Red de Enfermedades Raras (CIBERER), Universidade de Santiago de Compostela (USC), Santiago de Compostela, Spain

59. Department of Clinical Infection, Microbiology and Immunology, University of Liverpool Institute of Infection, Veterinary and Ecological Sciences , Liverpool, England, United Kingdom

60. Alder Hey Children's Hospital, Department of Infectious Diseases, Eaton Road, Liverpool, L12 2AP, United Kingdom

61. 2nd Department of Pediatrics, National and Kapodistrian University of Athens (NKUA), Children's Hospital "P, and A. Kyriakou", Athens, Greece

62. 1st Department of Infectious Diseases, Sotiria General Hospital, Athens, Greece

63. Pathology Department, University of Patras, General Hospital "Panagia i Voithia", Patras, Greece

64. Pathophysiology Department, Medical Faculty, National and Kapodistrian, Laiko General Hospital, University of Athens (NKUA), Athens, Greece

65. Translational and Clinical Research Institute, Newcastle University, Newcastle upon Tyne, United Kingdom

66. Great North Children's Hospital, Paediatric Immunology, Infectious Diseases & Allergy, Newcastle upon Tyne Hospitals NHS Foundation Trust, Newcastle upon Tyne, United Kingdom

67. NIHR Newcastle Biomedical Research Centre based at Newcastle upon Tyne Hospitals NHS Trust and Newcastle University, Westgate Rd, Newcastle upon Tyne NE4 5PL, United Kingdom

68. Great North Children's Hospital, Research Unit, Newcastle upon Tyne, United Kingdom

70. Population Health Sciences Institute, Newcastle University, Newcastle upon Tyne, United Kingdom

71. Great North Children's Hospital, Paediatric Oncology, Newcastle upon Tyne Hospitals NHS Foundation Trust, Newcastle upon Tyne, United Kingdom

72. Department of Infection & Tropical Medicine, Newcastle upon Tyne Hospitals NHS Foundation Trust, Newcastle upon Tyne, United Kingdom

73. NIHR Newcastle In Vitro Diagnostics Co-operative (Newcastle MIC), Newcastle upon Tyne, United Kingdom.

74. Servicio Madrileño de Salud (SERMAS),Pediatric Infectious Diseases Unit, Department of Pediatrics, Hospital Universitario 12 de Octubre, Madrid, Spain

75. Fundación Biomédica del Hospital Universitario 12 de Octubre (FIB-H12O), Unidad Pediátrica de Investigación y Ensayos Clínicos

(UPIC), Hospital Universitario 12 de Octubre, Instituto de Investigación Sanitaria Hospital 12 de Octubre (i+12), Madrid, Spain.

76. Universidad Complutense de Madrid, Faculty of Medicine, Department of Pediatrics, Madrid, Spain.

77. Amsterdam UMC, Emma Children's Hospital, Dept of Pediatric Immunology, Rheumatology and Infectious Disease, University of Amsterdam, The Netherlands

78. Sanquin, Dept of Molecular Hematology, University Medical Center, Amsterdam, The Netherlands

79. Infectious Disease Unit, Academic Department of Pediatrics, Bambino Gesù Children's Hospital, IRCCS, Rome 00165, Italy

80. Erasmus MC-Sophia Children's Hospital, Department of General Paediatrics, Rotterdam, The Netherlands

81. Erasmus MC-Sophia Children's Hospital, Department of Paediatric Infectious Diseases & Immunology, Rotterdam, The Netherlands

82. Erasmus MC, Department of immunology, Rotterdam, The Netherlands

83. Division of Infectious Disease, Department of Pediatrics, National Cheng Kung University Tainan, Taiwan

84. Riga Stradins University, Riga, Latvia

85. Children clinical university hospital, Riga, Latvia

86. Riga East clinical university hospital, Riga, Latvia

87. Service de Pédiatrie-Urgences, AP-HP, Hôpital Louis-Mourier, F-92700 Colombes, France

88. Université Paris Cité, Inserm, IAME, F-75018 Paris, France

89. BioMérieux - Open Innovation & Partnerships Department, Lyon, France

90. Department of Infectious diseases, University Medical Centre Ljubljana, Slovenia

91. University Children's Hospital, University Medical Centre Ljubljana, Slovenia

92. Faculty of Medicine, University of Ljubljana, Slovenia

94. Pediatric Infectious Diseases and Immunology, University Medical Center Utrecht, Utrecht, The Netherlands

95. Pediatric Intensive Care Unit, University Medical Center Utrecht, Utrecht, The Netherlands

96. Pediatric Rheumatology, University Medical Center Utrecht, Utrecht, The Netherlands

97. Pediatric Neonatal Intensive Care, Wilhelmina Children's Hospital, University Medical Center Utrecht, Utrecht, The Netherlands

98. Princess Maxima Center for Pediatric Oncology, Utrecht, The Netherlands

99. Department of Pediatrics, Inselspital, Bern University Hospital, University of Bern, Switzerland

100. Department of Intensive Care and Neonatology, and Children`s Research Center, University Children`s Hospital Zurich, Zurich, Switzerland

101. Child Health Research Centre, The University of Queensland, Brisbane, Australia

102. Department of Pediatrics, Inselspital, Bern University Hospital, University of Bern, Switzerland

103. Department of Intensive Care and Neonatology, and Children`s Research Center, University Children`s Hospital Zurich, Zurich, Switzerland

104. Child Health Research Centre, The University of Queensland, Brisbane, Australia

105. Clinic of Neonatology, Department Mother-Woman-Child, Lausanne University Hospital and University of Lausanne, Switzerland

106. Infectious Diseases Service, Department of Medicine, Lausanne University Hospital and University of Lausanne, Switzerland

107. Department of Pediatrics, Children's Hospital Lucerne, Lucerne, Switzerland

108. Pediatric Infectious Diseases Unit, Children's Hospital of Geneva, University Hospitals of Geneva, Geneva, Switzerland

109. Infectious Diseases and Vaccinology, University of Basel Children's Hospital, Basel, Switzerland

110. Children's Hospital Aarau, Aarau, Switzerland

111. Division of Infectious Diseases and Hospital Epidemiology, Children's Hospital of Eastern Switzerland St. Gallen, St. Gallen, Switzerland

112. Department of Neonatology, University Hospital Zurich, Zurich, Switzerland

113. Division of Infectious Diseases and Hospital Epidemiology, and Children's Research Center, University Children's Hospital Zurich, Switzerland

114. Children's Hospital Chur, Chur, Switzerland

115. Micropathology Ltd, The Venture Center, University of Warwick Science Park, Sir William Lyons Road, Coventry, CV4 7EZ,United Kingdom

116. Department of Pediatrics and Adolescent Medicine, Division of General Pediatrics, Medical University of Graz, Graz, Austria

117. Department of Pediatric Pulmonology, Medical University of Graz, Graz, Austria

118. Department of Pediatric Hematooncology, Medical University of Graz, Graz, Austria

119. Paediatric Intensive Care Unit, Medical University of Graz, Graz, Austria

120. University Clinic of Pediatrics and Adolescent Medicine Graz, Medical University Graz, Graz, Austria

121. Clinical Institute of Medical and Chemical Laboratory Diagnostics, Medical University Graz, Graz, Austria

122. Department of Internal Medicine, State Hospital Graz II, Location West, Graz, Austria

123. SkylineDx, Rotterdam, The Netherlands

124. Biobanking and BioMolecular Resources Research Infrastructure - European Research Infrastructure Consortium (BBMRI-ERIC), Neue Stiftingtalstrasse 2/B/6, 8010, Graz, Austria

125. Division of Pediatric Infectious Diseases, Department of Pediatrics, Dr. von Hauner Children's Hospital, University Hospital, LMU Munich, Munich, Germany

126. German Center for Infection Research (DZIF), Partner Site Munich, Munich, Germany

127. Department of Gynecology and Obstetrics, University Hospital, LMU Munich, Munich, Germany

128. Division of General Pediatrics, Department of Pediatrics, Dr. von Hauner Children's Hospital, University Hospital, LMU Munich, Munich, Germany

129. Division of Pediatric Haematology & Oncology, Department of Pediatrics, Dr. von Hauner Children's Hospital, University Hospital, LMU Munich, Munich, Germany

130. Division of Pediatric Rheumatology, Department of Pediatrics, Dr. von Hauner Children's Hospital, University Hospital, LMU Munich, Munich, Germany

131. Division of Pediatric Pulmonology, Department of Pediatrics, Dr. von Hauner Children's Hospital, University Hospital, LMU Munich, Munich, Germany

132. Division of Pediatric Gastroenterology, Department of Pediatrics, Dr. von Hauner Children's Hospital, University Hospital, LMU Munich, Munich, Germany

133. **Neonatal Intensive Care Unit, Department of Pediatrics, Dr. von Hauner Children's Hospital, University Hospital, LMU Munich, Munich, Germany**

134. **Paediatric Intensive Care Unit, Department of Pediatrics, Dr. von Hauner Children's Hospital, University Hospital, LMU Munich, Munich, Germany**

135. Department of Pediatric Cardiology and Pediatric Intensive Care, University Hospital, LMU Munich, Germany

136. Department of Paediatrics, St. Mary's Imperial College Hospital, London, United Kingdom

137. Department of Global Health and Development, Faculty of Public Health and Policy, London School of Hygiene and Tropical Medicine, London, United Kingdom

ISARIC consortium

ISARIC Comprehensive Clinical Characterisation Collaboration (ISARIC4C)

J Kenneth Baillie[3,13], Malcolm G Semple[138,139], Gail Carson[140], Peter JM Openshaw[141,142], Jake Dunning[141,143], Laura Merson[140], Clark D Russell[144], David Dorward[145], Maria Zambon[143], Meera Chand[146], Richard S Tedder[147,148,149], Saye Khoo[150], Lance CW Turtle[138,151], Tom Solomon[138,,152], Samreen Ijaz[143], Tom Fletcher[153], Massimo Palmarini[1], Antonia Ho[1], Emma C Thomson[1], Nicholas Price[155,156], Judith Breuer[157], Thushan de Silva[158], Chloe Donohue[159], Hayley Hardwick[138], Wilna Oosthuyzen[3], Miranda Odam[3], Primrose Chikowore[3], Lauren Obosi[3], Sara Clohisey[3], Andrew Law[3], Lucy Norris[160], Sarah Tait[161], Murray Wham[3], Richard Clark[162], Audrey Coutts[162], Lorna Donnelly[162], Angie Fawkes[162], Tammy Gilchrist[162], Katarzyna Hafezi[162], Louise MacGillivray[162], Alan Maclean[162], Sarah McCafferty[162], Kirstie Morrice[162], Lee Murphy[162], Nicola Wrobel[162], Sarah E McDonald[1], Victoria Shaw[163], Katie A. Ahmed[163], Jane A Armstrong[164], Lauren Lett[165], Paul Henderson[166], Louisa Pollock[167], Shyla Kishore[168], Helen Brotherton[169], Lawrence Armstrong[170], Andrew Mitra[171], Anna Dall[172], Kristyna Bohmova[173], Sheena Logan[173], Louise Gannon[174], Ken Agwuh[175], Srikanth Chukkambotla [176], Ingrid DuRand[177], Duncan Fullerton[178], Sanjeev Gar[179], Clive Graham[180], Tassos Grammatikopoulos[181,182], Stuart Hartshorn[183], Luke Hodgson[184], Paul Jennings[185], George Koshy[186], Tamas Leiner[186], James Limb[187], Jeff Little[188], Sheena Logan[188], Elijah Matovu[176], Fiona McGill[189], Craig Morris[190], John Morrice[191], David Price[192], Henrik Reschreiter[193], Tim Reynolds[190], Paul Whittaker[194], Thomas Jordan[169], Rachel Tayler[195], Clare Irving[196], Katherine Jack[196], Maxine Ramsay[197], Margaret Millar[197], Barry Milligan[198], Naomi Hickey[198], Maggie Connon[168], Catriona Ward[168], Laura Beveridge[191], Susan MacFarlane[174], Karen Leitch[169], Claire Bell[199], Lauren Finlayson[172], Joy Dawson[172], Janie Candlish[171], Laura McGenily[173], Tara Roome[183], Cynthia Diaba[200], Jasmine Player[201], Natassia Powell[202], Ruth Howman[183], Sara Burling[183], Sharon Floyd[184], Sarah Farmer[175], Susie Ferguson[203], Susan Hope[204], Lucy Rubick[193], Rachel Swingler[205], Emma Collins[206], Collette Spencer[189], Amaryl Jones[178], Barbara Wilson[207],

Diane Armstrong[208], Mark Birt[209], Holly Dickinson[190], Rosemary Harper[208], Darran Martin[210], Amy Roff[193], Sarah Mills[193].

138. NIHR Health Protection Research Unit, Institute of Infection, Veterinary and Ecological Sciences, Faculty of Health and Life Sciences, University of Liverpool, Liverpool, United Kingdom

139. Respiratory Medicine, Alder Hey Children's Hospital, Institute in The Park, University of Liverpool, Alder Hey Children's Hospital, Liverpool, United Kingdom

140. ISARIC Global Support Centre, Centre for Tropical Medicine and Global Health, Nuffield Department of Medicine, University of Oxford, Oxford, United Kingdom

141. National Heart and Lung Institute, Imperial College London, London, United Kingdom

142. Imperial College Healthcare NHS Trust: London, London, United Kingdom

143. National Infection Service, Public Health England, London, United Kingdom

144. Centre for Inflammation Research, The Queen's Medical Research Institute, University of Edinburgh, Edinburgh, United Kingdom

145. Edinburgh Pathology, University of Edinburgh, Edinburgh, United Kingdom

146. Antimicrobial Resistance and Hospital Acquired Infection Department, Public Health England, London, United Kingdom

147. Blood Borne Virus Unit, Virus Reference Department, National Infection Service, Public Health England, London, United Kingdom

148. Transfusion Microbiology, National Health Service Blood and Transplant, London, United Kingdom

149. Department of Medicine, Imperial College London, London, United Kingdom

150. Department of Pharmacology, University of Liverpool, Liverpool, United Kingdom

151. Tropical & Infectious Disease Unit, Royal Liverpool University Hospital, Liverpool, United Kingdom

152. Walton Centre NHS Foundation Trust, Liverpool, United Kingdom

153. Liverpool School of Tropical Medicine, Liverpool, United Kingdom

154. Department of Infectious Diseases, Queen Elizabeth University Hospital, Glasgow, Scotland, United Kingdom REMOVE

155. Centre for Clinical Infection and Diagnostics Research, Department of Infectious Diseases, School of Immunology and Microbial Sciences, King's College London, London, United Kingdom

156. Department of Infectious Diseases, Guy's and St Thomas' NHS Foundation Trust, London, United Kingdom

157. Division of Infection & Immunity, University College London and Great Ormond Street Hospital, London, United Kingdom

158. The Florey Institute for Host-Pathogen Interactions, Department of Infection, Immunity and Cardiovascular Disease, University of Sheffield, Sheffield, United Kingdom

159. Liverpool Clinical Trials Centre, University of Liverpool, Liverpool, United Kingdom

160. EPCC, University of Edinburgh, Edinburgh, Scotland, United Kingdom

161. Public Health Scotland, Glasgow, Scotland, United Kingdom

162. Edinburgh Clinical Research Facility, University of Edinburgh, Edinburgh, Scotland, United Kingdom

163. Institute of Translational Medicine, University of Liverpool, Liverpool, Merseyside, United Kingdom

164. Sheffield Teaching Hospitals, Sheffield, United Kingdom

165. University of Liverpool, Liverpool, United Kingdom

166. Royal Hospital for Children and Young People, Edinburgh, United Kingdom

167. Department of Paediatric Infectious Diseases and Immunology, Royal Hospital for Children, Glasgow, United Kingdom

168. Royal Aberdeen Children's Hospital, Aberdeen, United Kingdom

169. University Hospital Wishaw, North Lanarkshire, United Kingdom

170. Crosshouse & Ayr Hospital, Kilmarnock, Scotland, United Kingdom

171. Dumfries & Galloway Royal Infirmary, Dumfries, United Kingdom

172. Borders General Hospital, Melrose, United Kingdom

173. Forth Valley Royal Hospital, Larbert, United Kingdom

174. Tayside Children's Hospital, Ninewells Hospital, NHS Tayside, Dundee, United Kingdom, Ninewells Hospital, NHS Tayside, Dundee, United Kingdom

175. Doncaster and Bassetlaw Teaching Hospitals NHS Foundation Trust, Doncaster, United Kingdom NHS Foundation Trust, Doncaster, United Kingdom

176. Burnley General Teaching Hospital, Burnley, United Kingdom

177. Hereford County Hospital, Hereford, United Kingdom

178. Leighton Hospital, Leighton, United Kingdom

179. Walsall Healthcare NHS Trust, Walsall, United Kingdom

180. Cumberland Infirmary, Cumberland, United Kingdom

181. Paediatric Liver, GI & Nutrition Centre and MowatLabs, King's College Hospital, London, United Kingdom

182. Institute of Liver Studies, King's College London, London, United Kingdom

183. Birmingham Women's Children's Hospital, Birmingham, United Kingdom

184. St Richards' Hospital, Chichester, United Kingdom

185. Airedale General Hospital, Keighley, United Kingdom

186. Hinchingbrooke Hospital, Huntingdon, United Kingdom

187. Darlington Memorial Hospital, Darlington, United Kingdom

188. Warrington Hospital, Kilmarnock, United Kingdom

189. Leeds Teaching Hospitals NHS Trust, Leeds, United Kingdom

190. Queens Hospital Burton, Burton-on-Trent, United Kingdom

191. Queen Margaret Hospital, Dunfermline, United Kingdom

192. Royal Victoria Infirmary, Newcastle upon Tyne, United Kingdom

193. Poole University Hospital, Dorset, United Kingdom

194. Bradford Royal infirmary, Bradford, United Kingdom

195. Department of Paediatric Gastroenterology, Hepatology and Nutrition, Royal Hospital for Children, Glasgow, United Kingdom

196. Avon and Wiltshire Mental Health Partnership NHS Trust, Bath, United Kingdom

197. Royal Hospital For Children and Young People, Edinburgh, United Kingdom

198. Queen Elizabeth University Hospital, Glasgow, United Kingdom

199. University Hospital Crosshouse, Kilmarnock, United Kingdom

200. Royal Free Hospital, London, United Kingdom

201. Diana Princess of Wales Hospital, Grimsby, United Kingdom

202. King's College Hospital, London, United Kingdom

203. Western General Hospital, Edinburgh, United Kingdom

204. Barnsley Hospital, Barnsley, United Kingdom

205. Bradford Teaching Hospitals NHS Foundation Trust, Bradford, United Kingdom

206. Wye Valley NHS Trust, Hereford, United Kingdom

207. Newcastle upon Tyne Hospitals NHS Foundation Trust, Newcastle upon Tyne, United Kingdom

208. West Cumberland Hospital, Whitehaven, United Kingdom

209. University Hospital of North Durham, Durham, United Kingdom

210. Worthing Hospital, Worthing, United Kingdom

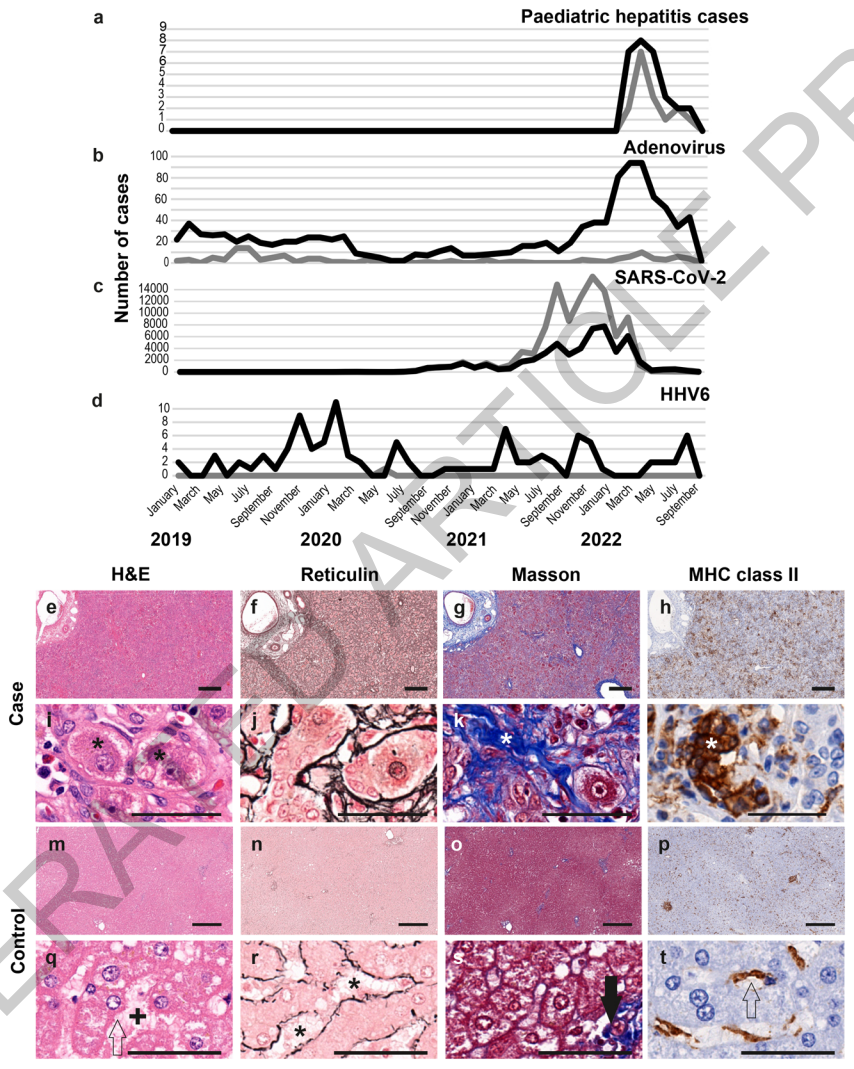

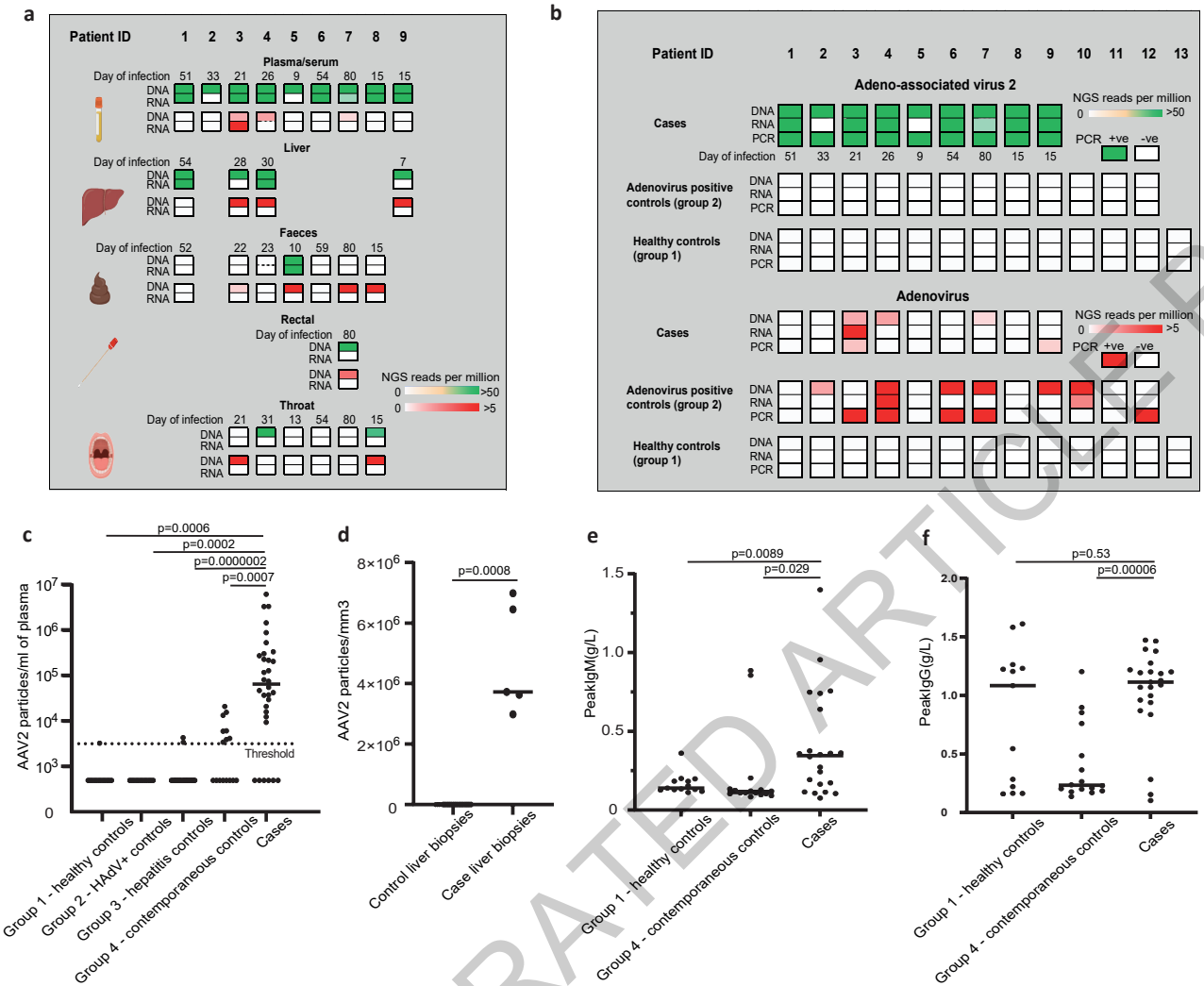

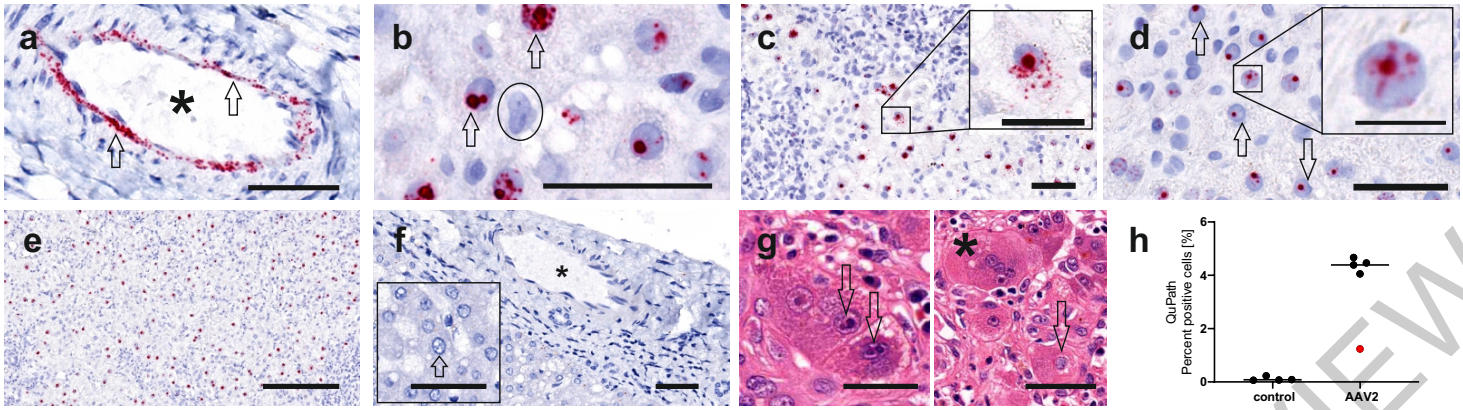

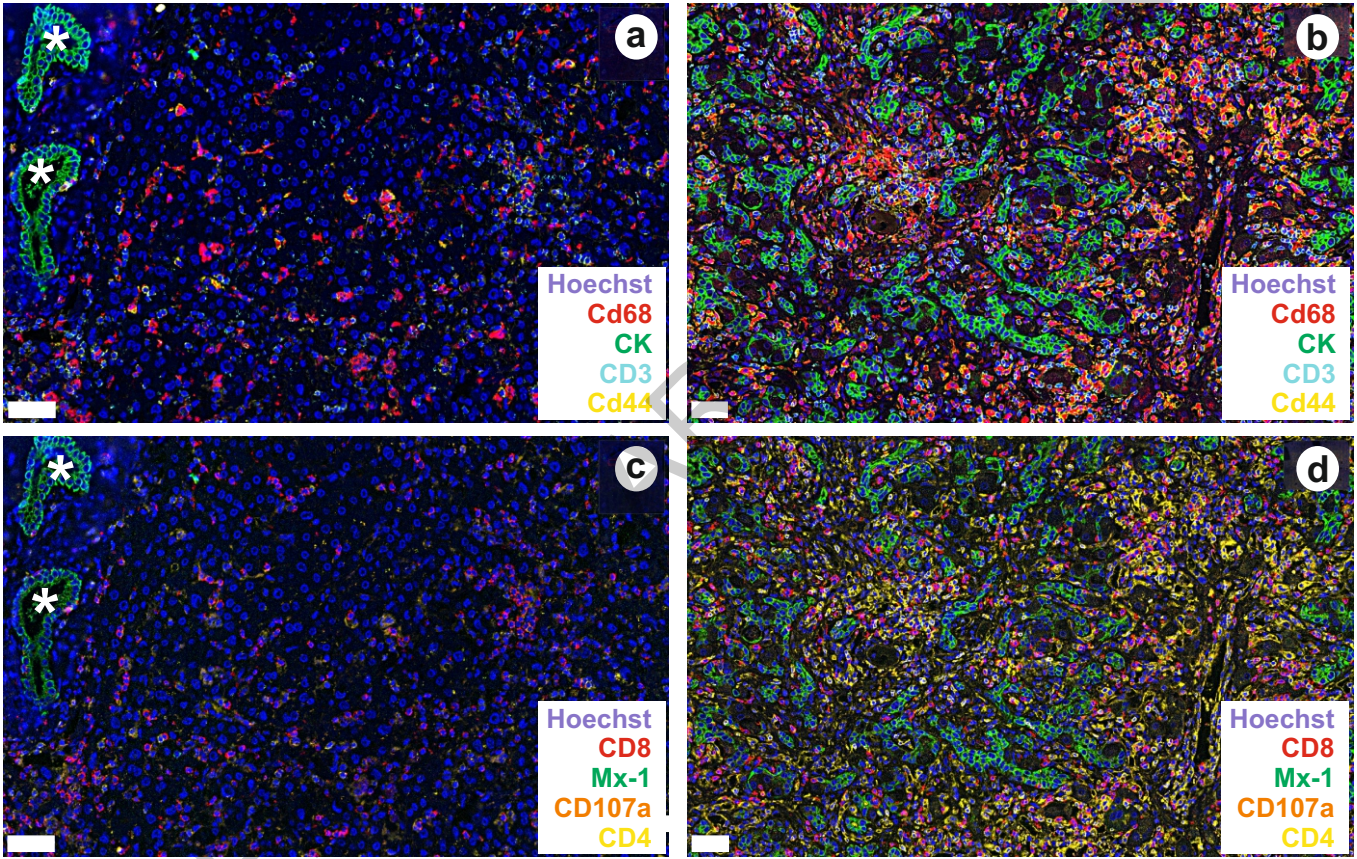
a
Hoechst
Cd68
CK
CD3
Cd44
b
Hoechst
Cd68
CK
CD3
Cd44
c
Hoechst
CD8
Mx-1
CD107a
CD4
d
Hoechst
CD8
Mx-1
CD107a
CD4

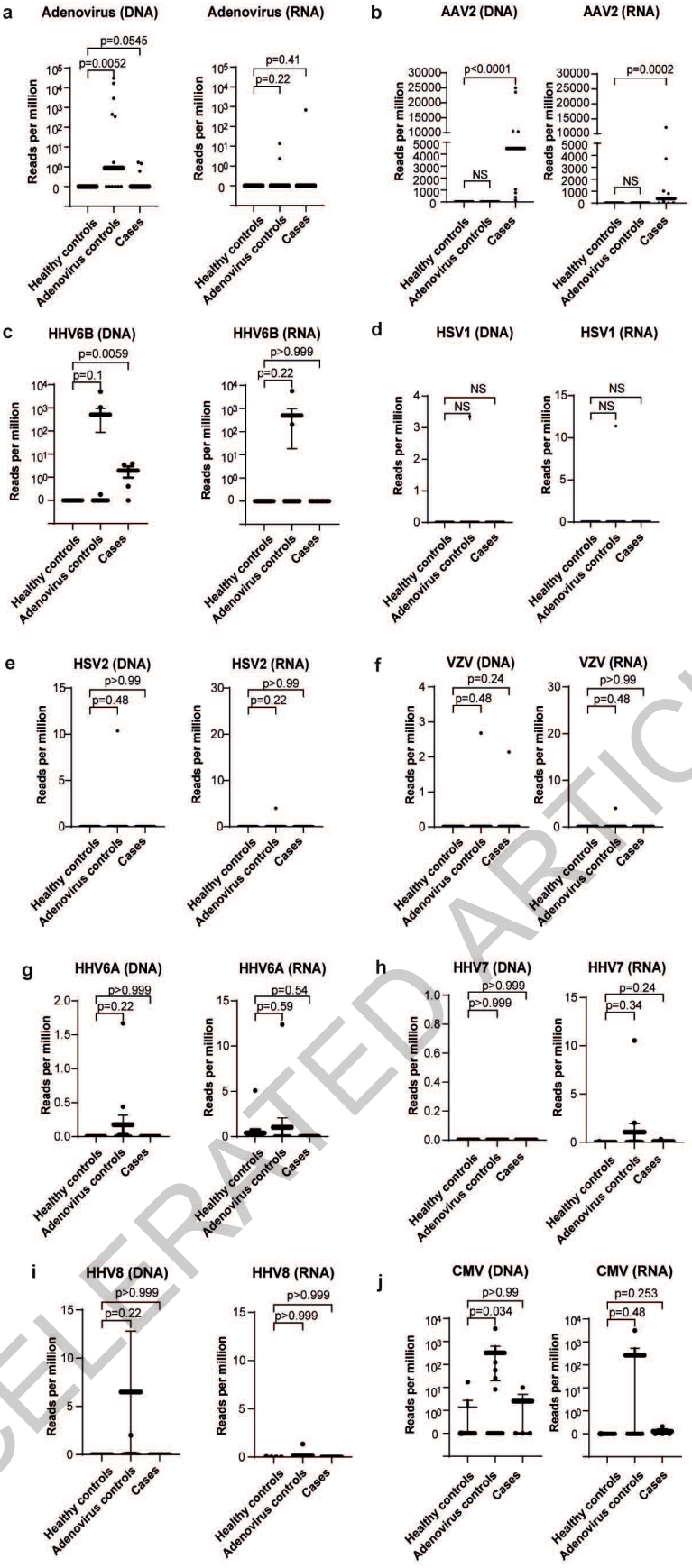

Extended Data Fig. 1

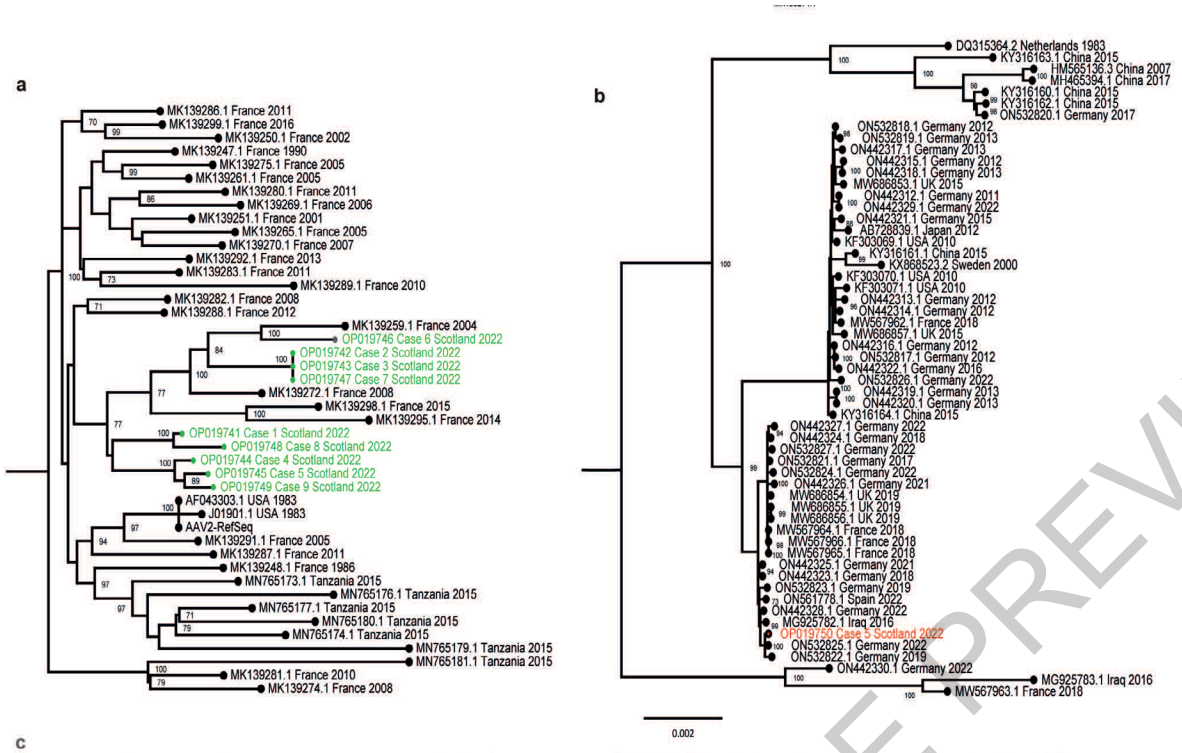

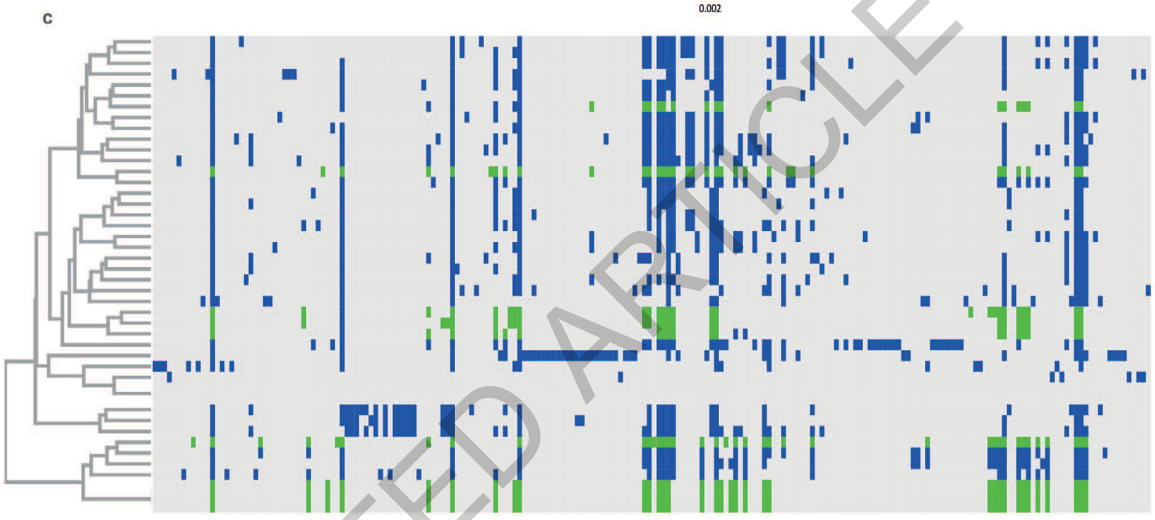

d

Mutation	Protein	% Cases	% Published
V151A	VP1-3	89	50
Q164N	VP1-3	67	35
R447K	VP1-3	56	6
T450A	VP1-3	56	6
Q457M	VP1-3	100	12
S492A	VP1-3	100	62
E499D	VP1-3	100	15
P521T	VP1-3	89	6
F533Y	VP1-3	100	12
R585S	VP1-3	100	91
R588T	VP1-3	100	94

Mutation	Protein	% Cases	% Published
Q6P	AAP	100	91
E70A	AAP	89	50
P73L	AAP	89	74
T80I	AAP	100	74
S81C	AAP	100	59
N83S	AAP	89	88
K84R	AAP	67	76
I95T	AAP	100	91
L103P	AAP	56	56
F116S	AAP	67	24
H117P	AAP	67	12
D132G	AAP	67	44

Mutation	Protein	% Cases	% Published
T183A	Rep 78, 52	100	94
V508A	Rep 78, 52	100	82
L609V	Rep 78, 52	89	12
F619S	Rep 78, 52	100	94

Extended Data Fig. 2

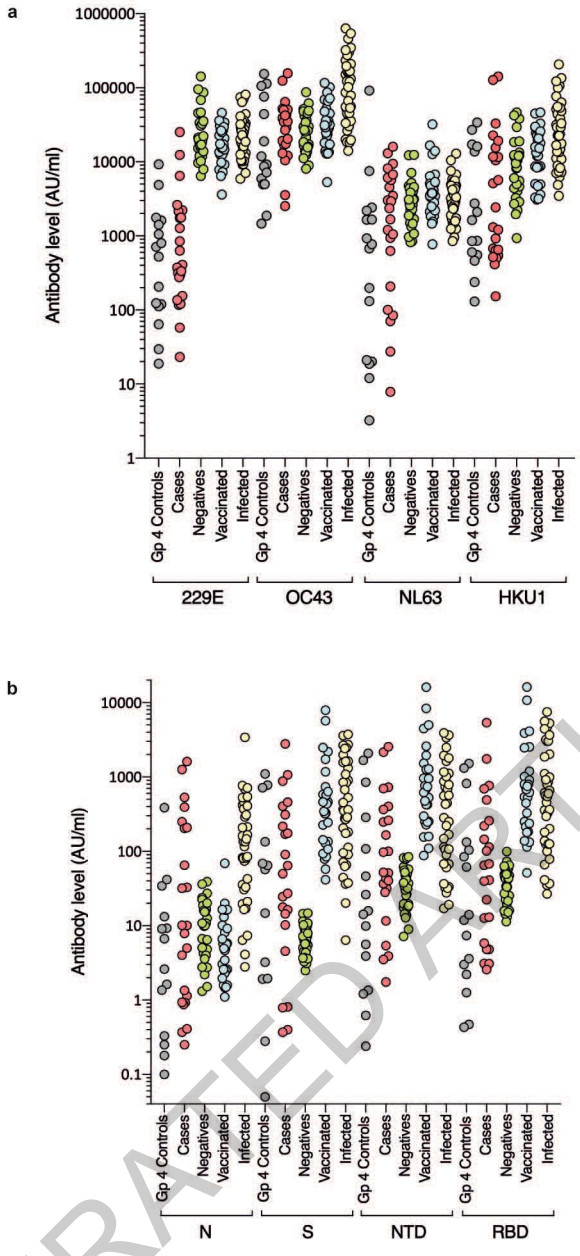

Extended Data Fig. 3

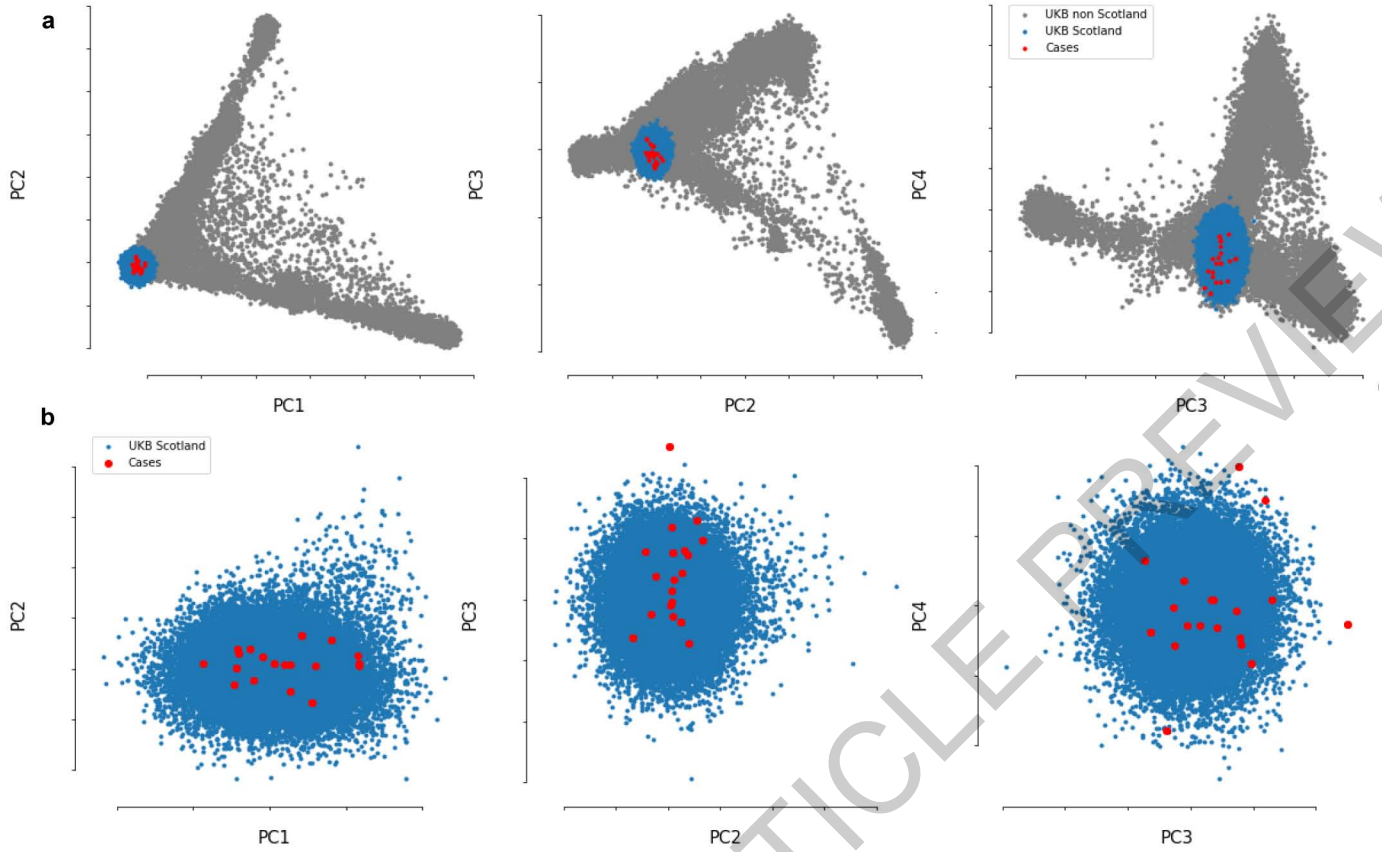

Extended Data Fig. 4

	CVR1	CVR3	CVR4	CVR9	CVR35
Modified Ishak score	6/18	10/18	10/18	8/18	11/18
Portal inflammation	2/4	4/4	4/4	2/4	2/4
Interface hepatitis	2/4	4/4	4/4	4/4	4/4
Confluent necrosis	0/6	0/6	0/6	0/6	1/6
Lobular inflammation	2/4	2/4	2/4	2/4	4/4

Extended Data Table 1

a

	Cases - metagenomic & TE sequencing analysis (n=9)	**Controls**			
		Group 1 DIAMONDS Healthy (n=13)	P value*	Group 2 DIAMONDS HAdV infection with normal transaminases (N=12)	P value*
Sex - male	4 (44.4)	10 (76.9)	0.19	7 (58.3)	0.67
Age (years)	3.9 (3.4-5.1)	4.1 (3.6-4.8)	0.87	1.4 (1.1-3.1)	0.0006
Recruitment period	14 March – 20 April 2022	6 Nov 2020 - 6 Jul 2021	-	22 May 2020 - 22 Dec 2021	-

b

	Cases – PCR (n=32)	**Controls**							
		Group 1 DIAMONDS Healthy (n=13)	P value*	Group 2 DIAMONDS HAdV infection with normal transaminases (N=12)	P value*	Group 3 DIAMONDS Elevated transaminases with no HAdV infection (n=33)	P value*	Group 4 Scottish hospitalised controls (n=16)	P value*
Sex - male	11 (34.4)	10 (76.9)	0.019	7 (58.3)	0.18	17 (51.5)	0.21	-	-
Age (years) †	4.1 (2.7-5.5)	4.1 (3.6-4.8)	0.95	1.4 (1.1-3.1)	0.0002	10.2 (7-13.6)	<0.0001	-	-
Recruitment period	14 March – 20 August 2022	6 Nov 2020 - 6 Jul 2021	-	22 May 2020 - 22 Dec 2021	-	9 Sep 2020 - 8 Jan 2022	-	12 March - 4 April 2022	-

Extended Data Table 2

nature portfolio

Corresponding author(s): Emma Thomson

Last updated by author(s): Dec 14, 2022

Reporting Summary

Nature Portfolio wishes to improve the reproducibility of the work that we publish. This form provides structure for consistency and transparency in reporting. For further information on Nature Portfolio policies, see our Editorial Policies and the Editorial Policy Checklist.

Statistics

For all statistical analyses, confirm that the following items are present in the figure legend, table legend, main text, or Methods section.

n/a	Confirmed
☐	☒ The exact sample size (*n*) for each experimental group/condition, given as a discrete number and unit of measurement
☐	☒ A statement on whether measurements were taken from distinct samples or whether the same sample was measured repeatedly
☐	☒ The statistical test(s) used AND whether they are one- or two-sided *Only common tests should be described solely by name; describe more complex techniques in the Methods section.*
☒	☐ A description of all covariates tested
☐	☒ A description of any assumptions or corrections, such as tests of normality and adjustment for multiple comparisons
☐	☒ A full description of the statistical parameters including central tendency (e.g. means) or other basic estimates (e.g. regression coefficient) AND variation (e.g. standard deviation) or associated estimates of uncertainty (e.g. confidence intervals)
☐	☒ For null hypothesis testing, the test statistic (e.g. *F*, *t*, *r*) with confidence intervals, effect sizes, degrees of freedom and *P* value noted *Give P values as exact values whenever suitable.*
☒	☐ For Bayesian analysis, information on the choice of priors and Markov chain Monte Carlo settings
☒	☐ For hierarchical and complex designs, identification of the appropriate level for tests and full reporting of outcomes
☒	☐ Estimates of effect sizes (e.g. Cohen's *d*, Pearson's *r*), indicating how they were calculated

Our web collection on statistics for biologists contains articles on many of the points above.

Software and code

Policy information about availability of computer code

Data collection

No commercial code was used for data collection in this study

Data analysis

HLA ANALYSIS
The Bridging ImmunoGenomic Data-Analysis Workflow Gaps (BIGDAWG) R package to derive OR and corrected p values for individual HLA alleles.30 Bonferroni corrected p value significance threshold, adjusted for multiple comparisons (168 HLA alleles), was p < 3.0×10−4.

BIOINFORMATICS ANALYSIS
Reads for each sample were first quality checked, Illumina adapters were trimmed using Trim Galore version 0.6.6 (https://github.com/FelixKrueger/TrimGalore), and reads were then mapped to the human genome using BWA-MEM version 0.7.17 (https://github.com/lh3/bwa). Only reads that did not map to the human genome were used for metagenomic analyses. Non-human reads were then de novo assembled using MetaSPAdes version 3.15.5 (https://github.com/ablab/spades) to generate contigs for each sample. Contigs were then compared against a protein database of all NCBI RefSeq organisms (including virus, bacteria, eukaryotes) with BLASTX using DIAMOND version 2.0.15 (https://github.com/bbuchfink/diamond). In addition, non-human reads for each sample were aligned to a small panel of HAdV NCBI RefSeq genomes (HAdV-A, B1, B2, C, D, E, F, 1, 2, 5, 7, 35, 54 as well as HAdV-F41).

STATISTICAL ANALYSIS
Differences between cases and control groups were tested using Fisher's Exact Test for categorical variables and Mann-Whitney (two tailed) for continuous variables. Spearman's rank correlation coefficients were calculated for the relationships between the trajectories of viral load and ALT and bilirubin. We used R studio version 1.2.5033, R version 4.1.2 and GraphPad version 9.0.0 for most statistical analyses. For coronavirus serology experiments, comparisons were carried out with one way ANOVA and Tukey's Multiple Comparison test, carried out in

GraphPad version 8.4.3.

For manuscripts utilizing custom algorithms or software that are central to the research but not yet described in published literature, software must be made available to editors and reviewers. We strongly encourage code deposition in a community repository (e.g. GitHub). See the Nature Portfolio guidelines for submitting code & software for further information.

Data

Policy information about availability of data

All manuscripts must include a data availability statement. This statement should provide the following information, where applicable:

- Accession codes, unique identifiers, or web links for publicly available datasets
- A description of any restrictions on data availability
- For clinical datasets or third party data, please ensure that the statement adheres to our policy

Datasets generated in the current study are appended as Source Data, Extended Data Tables and Supplementary Tables. Data, protocols, and all documentation around this analysis may be made available to academic researchers after authorisation from the independent data access and sharing committee. Clinical data and analysis scripts are available on request to the Independent Data Management and Access Committee at https://isaric4c.net/ sample_access. Restrictions apply to the availability of identifiable clinical data. Due to the relatively small number of cases, de-aggregation of data is potentially disclosive, as is the patient-level line list data. Therefore, a formal data sharing agreement is required for data access. The Independent Data and Material Access Committee considers requests as they arrive; most responses are made within 28 days. Use of clinical samples are also restricted under ethical approvals obtained for their use. Genome sequences are available in GenBank with accession numbers for AAV2: OP019741-OP019749 and for HAdV-F41: OP019750.

Human research participants

Policy information about studies involving human research participants and Sex and Gender in Research.

Reporting on sex and gender	For the case control study, recruited patients were female (n=20) and male (n=12). Group 1 healthy control subjects were restricted to 13 children recruited in the UK between January 2020 and April 2022 and were age-matched but not sex-matched due to availability of samples (10 male, 3 female; age range 3-5 years). Group 2 subjects were children (8 male, 4 female; age range 1-4 years) with PCR-confirmed HAdV infection and normal transaminases Group 3, 33 children (18 male, 15 female; age range 2-16 years) with raised transaminases who were HAdV PCR negative. Group 4 included 16 residual samples from children from the NHS GG&C biorepository aged <18 years. Further information was not available under ethical protocols for the use of residual biorepository samples. For the HLA analysis a further 3 cases were recruited to the ISARIC CCP-UK cohort and had HLA typing carried out but further clinical samples and additional clinical data were not available.
Population characteristics	The median age of affected patients was 4.1 years (IQR: 2.7 to 5.5 years) (Table 1). Twenty of the 32 (63%) children were female, and all were of white ethnicity. Eighteen (56%) of the children reported a subacute history 2-12 weeks prior to acute hepatitis, characterised by an initial gastroenteritis-like illness followed by intermittent vomiting, abdominal pain and fatigue. Most of the affected children (23/32) had no other medical conditions: one child had previously received a liver transplant; none of the other cases were immunocompromised and none had received COVID-19 vaccination. All routine blood tests for viral hepatitis, including hepatitis A, B, C, E, acute Epstein-Barr virus (EBV), cytomegalovirus (CMV), human herpes virus (HHV) 6/7 and herpes simplex virus (HSV) were negative
Recruitment	To investigate the aetiology of the acute hepatitis cases, we recruited 32 of the earliest affected children who presented to hospital between 14 March and 4 April 2022 into the International Severe Acute Respiratory and Emerging Infections Consortium (ISARIC) WHO Clinical Characterisation Protocol UK (CCP-UK) [ISRCTN 66726260]7. All cases who fulfilled the case definition and were willing to participate were recruited. For the HLA analysis a further 3 cases were recruited to the ISARIC CCP-UK cohort and had HLA typing carried out but further clinical samples and additional clinical data were not available. Control samples (Groups 1,2 and 3) were obtained from the Diagnosis and Management of Febrile Illness using RNA Personalised Molecular Signature Diagnosis study cohort (DIAMONDS; https://www.diamonds2020.eu). This study recruited children presenting with suspected infection or inflammation. Patients were recruited with the informed written consent of parents or guardians.
Ethics oversight	32 affected children, who presented to hospital between 14 March and 20 August 2022 and who met the PHS case definition into the International Severe Acute Respiratory and Emerging Infections Consortium (ISARIC) WHO Clinical Characterisation Protocol UK (CCP-UK) [ISRCTN 66726260].7 Ethical approval was given by the South Central–Oxford C Research Ethics Committee in England (13/SC/0149), the Scotland A Research Ethics Committee (20/SS/0028), and the WHO Ethics Review Committee (RPC571 and RPC572). Control samples (Groups 1-3) were obtained from the Diagnosis and Management of Febrile Illness using RNA Personalised Molecular Signature Diagnosis study cohort (DIAMONDS; https://www.diamonds2020.eu). Patients were recruited with the written informed consent of parents or guardians. Contemporaneous Scottish surplus plasma and liver biopsy control samples (Control Group 4) from the Diagnostic Pathology/ Blood Sciences archive were obtained with NHS GG&C Biorepository approval (application #717; REC 22/WS/0020). These samples were used without consent following HTA legislation on consent exemption. Genetic (HLA) control data was obtained using the UK Biobank Resource (project 788; 21/NW/0157). Participants in the UK Biobank have been recruited with written informed consent.

Note that full information on the approval of the study protocol must also be provided in the manuscript.

Field-specific reporting

Please select the one below that is the best fit for your research. If you are not sure, read the appropriate sections before making your selection.

☒ Life sciences ☐ Behavioural & social sciences ☐ Ecological, evolutionary & environmental sciences

For a reference copy of the document with all sections, see nature.com/documents/nr-reporting-summary-flat.pdf

Life sciences study design

All studies must disclose on these points even when the disclosure is negative.

Sample size	All available cases were selected. All available healthy control samples that could be age-matched to cases were obtained from the DIAMONDS cohort (we planned for up to a 1-3:1 ratio of controls:cases). We selected all available control subjects in group 2 (HAdV positive with normal LFTs) from the DIAMONDS cohort. These were all children but were not age matched. We also selected all available control subject samples in group 3 (hepatitis of alternative aetiology) from the DIAMONDS cohort. We used all available residual samples from children from the same time period as cases in group 4.
Data exclusions	We excluded any cases that did not meet the PHS definition for non-A-E paediatric hepatitis on the basis of age (over 10 years of age or with an alternative diagnosis or from whom clinical data was not available). We excluded 5 plasma samples in the case control study from the NGS analysis of herpesviruses because during nucleic extraction in the relevant clinical laboratory, murine cytomegalovirus (CMV) had been used as an extraction control. This was not used for other sample extractions in the case control study. Clinical specimens taken from cases (throat, rectal swab, faeces and liver samples) also had murine CMV added to the samples and were also excluded from the NGS herpes read count analysis. However, all samples were tested for human herpesviruses by PCR.
Replication	PCR experiments were carried out in triplicate, other than GAPDH PCR which was carried out in duplicate or triplicate. Results were highly concordant. There were four AAV2 Ct values that were borderline (traversing the limit of detection). These were considered negative as weakly positive results were not reproducible and read counts for all samples were negative by metagenomic and target enrichment NGS. Next generation sequencing experiments were repeated on separate runs using different methods (metagenomic sequencing and then semi-agnostic target enrichment sequencing). Results were also confirmed by PCR for AAV2, HAdV and HHV6.
Randomization	As described above, all available cases were selected. All available healthy control samples that could be age-matched to cases were obtained from the DIAMONDS cohort (we planned for up to a 1-3:1 ratio of controls:cases). We selected all available control subjects in group 2 (HAdV positive with normal LFTs) from the DIAMONDS cohort. These were all children but were not age matched. We also selected all available control subject samples in group 3 (hepatitis of alternative aetiology) from the DIAMONDS cohort.
Blinding	The first sequencing run was of samples from 5 cases carried out urgently at the request of Public Health Scotland and investigators were not blinded to these as ethical permissions were not in place for the use of control samples. Subsequent runs were carried out when control samples were available and included 4 further cases. These were analysed with blinding of case/control status and then samples were compared to look for viruses present in cases and controls. PCR, serology and histology experiments were carried out with blinding in place.

Reporting for specific materials, systems and methods

We require information from authors about some types of materials, experimental systems and methods used in many studies. Here, indicate whether each material, system or method listed is relevant to your study. If you are not sure if a list item applies to your research, read the appropriate section before selecting a response.

Materials & experimental systems

n/a	Involved in the study
☐	☒ Antibodies
☒	☐ Eukaryotic cell lines
☒	☐ Palaeontology and archaeology
☒	☐ Animals and other organisms
☒	☐ Clinical data
☒	☐ Dual use research of concern

Methods

n/a	Involved in the study
☒	☐ ChIP-seq
☒	☐ Flow cytometry
☒	☐ MRI-based neuroimaging

Antibodies

Antibodies used	For AAV2 ELISA, bound human antibody was detected with either anti-human IgM or anti-human IgG (Merck, UK cat no. A9794 and A1543, respectively). Antibodies for IHC are listed below. AAntigen Dilution Clone Product code, company Antigen retrieval Detection system

MHCII 1:200 none M0746, Dako/Agilent Pressure cooking; citrate pH6 Envision Dako Agilent
C4d complement 1:100 none Quidel A213 Antihuman C4d ER2 (20) Leica BOND polymer DS9800 and BOND DAB enhancer
CD3 1:100 LN10 Leica NCL-L-CD3-565 ER2 (20) Leica BOND polymer DS9800 and BOND DAB enhancer
CD4 1:200 1F6 Leica NCL-L-CD4-368 ER2 (20) Leica BOND polymer DS9800 and BOND DAB enhancer
CD8 1:50 4B11 Leica NCL-CD8-4B11 ER2 (20) Leica BOND polymer DS9800 and BOND DAB enhancer
CD20 1:200 L26 Novocastra NCL-L-CD20-L26 ER1 (20) Leica BOND polymer DS9800 and BOND DAB enhancer

Target Ref # Supplier Reporter/Barcode Fluorophore Concentration
CD20 4450018 Akoya Biosciences Bx007 AF750 1/200
CD44 4450041 Akoya Biosciences Bx005 Atto 550 1/100
CD3 4450030 Akoya Biosciences Bx045 Cy5 1/200
PanCK 4450020 Akoya Biosciences Bx019 AF750 1/200
CD31 4450017 Akoya Biosciences Bx001 AF750 1/100
Mx1 M143 Custom made- University Medical Centre Freiburg Bx022 AF 750 1/50
CD8 4250012 Akoya Biosciences BX026 Atto 550 1/200
CD68 4350019 Akoya Biosciences Bx015 Cy5 1/200
CD107a 4350001 Akoya Biosciences Rx006 Cy5 1/200
CD4 4350018 Akoya Biosciences Bx003 cy5 1/200

Validation

For IHC, C4d was validated on Kidney with acute rejection versus normal kidney tissue. Validation policies and procedures were carried out in accordance with ISO accreditation ISO 15189. CD3, CD4, CD8 and CD20 were validated with normal tonsil control tissue and positive case tissue (lymphoma) from a minimum of 3 cases. Procedures were carried out in accordance with ISO 15189. Test subject tissue for these cases was compared with normal controls and negative controls.
For the CODEX analysis, we carried out validation of antibodies by 1.) replacing the primary antibody with isotype serum and 2.) checking in each section that stained cells had the morphology of the cell to be stained, e.g. MHCII macrophage-like cells close to the sinus using concentrations, as recommended by the manufacturer.